LBL-14219

Lawrence Berkeley Laboratory
UNIVERSITY OF CALIFORNIA

ENERGY & ENVIRONMENT DIVISION

BIOCONVERSION OF CELLULOSE

Charles R. Wilke and Harvey W. Blanch

March 1982

Prepared for the U.S. Department of Energy under Contract DE-AC03-76SF00098

DISCLAIMER

Printed in the United States of America
Available from
National Technical Information Service
U.S. Department of Commerce
5285 Port Royal Road
Springfield, VA 22161
Price Code: A06

LBL-14219

LBL--14219

DE82 014949

BIOCONVERSION OF CELLULOSE

DEPARTMENT OF ENERGY
DIVISION OF BASIC ENERGY SCIENCES

Charles R. Wilke
Harvey W. Blanch
Lawrence Berkeley Laboratory
Department of Chemical Engineering
University of California
Berkeley, California 94720

Work Progress Report FY 1981

This work was supported by the Director, Office for Energy Research, Office of Basic Energy Sciences, Division of Chemical Science Processes and Techniques Branch of the U.S. Department of Energy under Contract DE-AC03-76SF00098.

BIOCONVERSION OF CELLULOSE

TABLE OF CONTENT

I. STUDIES OF THE MECHANISM AND KINETICS OF CELLULOSE HYDROLYSIS

A. Kinetics and Mechanistic Studies on Cellulase Enzymes

1. Introduction

Most studies of enzyme kinetics have been concerned with heterogeneous systems: the action of soluble enzymes on soluble substrates. Studies of homogeneous enzyme kinetics have been largely confined to the action of insoluble (immobilized) enzymes and soluble substrates. Much less research has been conducted on the action of soluble enzymes on insoluble substrates. The enzymatic hydrolysis of cellulose falls in this latter area, and thus is of concern, not only for its applications in saccharification technology, but also as an investigation into this lesser-known area of enzyme kinetics.

The kinetics of enzymatic hydrolysis of cellulose depends on the structural features of cellulose, the nature of the enzyme system, and the interaction of substrate and enzyme. Structural features pertinent to the development of a model for cellulose hydrolysis include particle size and degree of crystallinity. These influence both the surface available for enzyme binding and the rate of reaction, since amorphous regions are degraded readily, while hydrolysis of crystalline regions proceeds only slowly. The nature of the cellulase system is described by the relative amounts of the constituent enzymes--endoglucanases, exoglucohydrolases, cellobiohydrolases and β-glucosidases. The interaction of substrate and enzymes is described by adsorption, reaction, and product inhibition phenomena. A mechanistic model incorporating all of these three groups of factors has not yet

been developed, and is the objective of this work.

2. Current Research

a. Enzyme purification

The scheme for the purification of components of the cellulase complex obtained from Trichoderma reesei has been developed in modified form, as shown in Figure IA-1. This scheme is similar to that previously described except for changes in composition of eluting buffers made to optimize the separation, and added steps to remove salts which can interfere with separation. Results of the ion exchange step are shown in Figure IA-2 (second step of the purification scheme). Results of gel permeation chromatography of the cellobiohydrolase demonstrate that this component was purified to homogeneity.

b. Cellobiohydrolase activity determination

Previously shown specific activity determinations of partially purified components indicate a decrease in specific activity of cellobiohydrolase with each stage of the purification. This is not due to a decrease in intrinsic activity of this protein, but a result of the synergistic action of components on highly crystalline substrates. Recovery of full activity with recombination of purified components demonstrates this point. To show that steps in the purification scheme are valid not only in obtaining protein homogeneous in physical properties, but in enzymatic action as well, an assay needs to be devised to demonstrate increases in specific activity concomitant with each stage of purification of protein, as is the case with the other components of the cellulase complex. To this end,

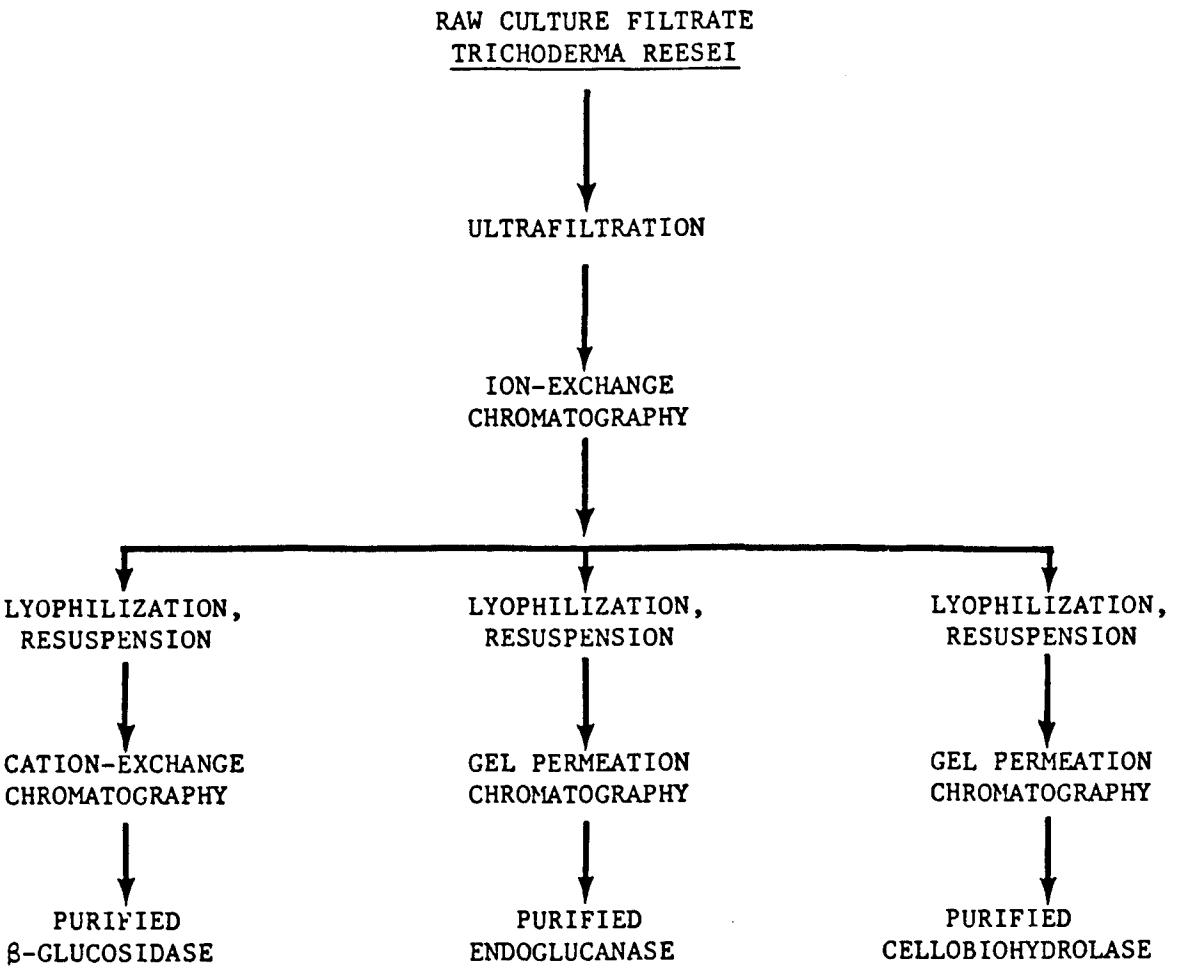

PURIFICATION OF CELLULASE COMPONENTS

XBL 8111-12529B

Figure 1A-1

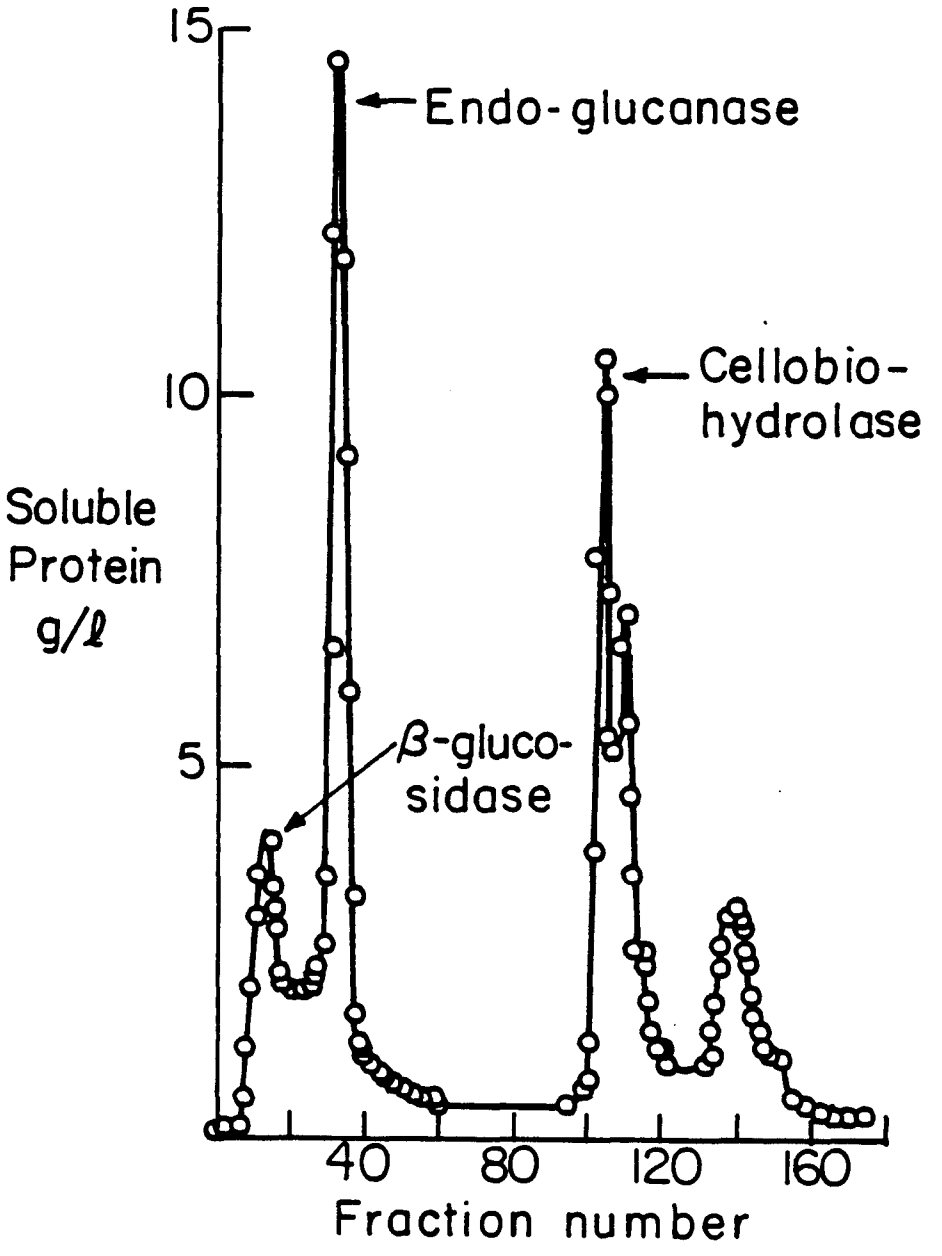

ION-EXCHANGE CHROMATOGRAPHY OF CELLULASE COMPONENTS

XBL 8111-12529A

Figure 1A-2

assay of cellobiohydrolase activity by measuring formation of cellobiose from phosphoric acid swollen (amorphous, Walseth cellulose) is being substituted for traditional measurement of reducing sugar formation from cotton (crystalline cellulose). This is consistent with new knowledge of the mechanism of action of cellulase components, corresponding to the specificity of enzyme action, rather than C_1 (cotton) and C_x (soluble cellulose derivative) measurements which do not correspond to a specific enzyme action but of combined action of several components. Details of this procedure are being developed, using the enzymatic conversion of cellobiose to glucose for use on a glucose analyzer.

3. Future Research

Determination of Langmuir isotherms for the adsorpion of purified endoglucanase and purified cellobiohydrolase separately, and in varying proportions, is the first step in developing a model to describe the interaction of enzyme and substrate. This has not been done previously for enzyme from this source except with the raw culture filtrate containing a constant proportion of the two enzymes.

Kinetic and inhibition constants for the action of β-glucosidase, and association constants for glucose-endoglucanase and cellobiose- cellobiohydrolase, will be obtained from kinetic studies on the action of β-glucosidase in the presence of variable amounts of cellobiohydrolase, endoglucanase, cellobiose, and glucose. This will characterize the homogeneous reactions in enzymatic hydrolysis of cellulose

and, in conjunction with adsorption data will comprise the kinetic model being devised.

B. International Cooperative Measurement of Cellulase Enzyme Activity

1. Introduction

In 1976, the Biotechnology Commission of the International Union of Pure and Applied Chemistry (IUPAC) recommended analysis of areas of microbial technology relating to energy and chemicals from renewable resources. Following subsequent meetings, task objectives were proposed in the areas of: 1) photosynthesis and efficiency, 2) hydrogen production, 3) cellulase production and measurement, 4) saccharification, 5) single cell protein production and measurement, 6) Biomass substrates and definition, 7) yields, balances, and net energetics of biomass (hexosans and pentosans) to ethanol. During these meetings it became clear that there was a great need for clear, reproducible and appropriate methodologies for cellulase enzyme assays, cell and protein yields, maintenance, productivities and rational evaluation of substrates which would be broadly applicable for those doing research in the field of bioconversion of renewable resources. It was further proposed that currently scattered data when compiled in a critical way, would enable scientists and engineers to use and compare the methods in their research and development studies and acquire by concensus a series of suitable methodologies. Lastly, it was also proposed that IUPAC publish a comprehensive document on these questions and solutions for the benefit of those in this field.

2. Current Research

This group was invited to participate in the submission of various enzyme assays used in our laboratory. In addition, the preliminary combined report to the IUPAC Biotechnology Commission was critically reviewed by us as well as by most of the participating groups.

In biomass conversion, the area of enzyme assay has been somewhat of a controversy. The large spread in ratios of constituents, protein content and activities in reported values results from a number of unfortunately diverging factors. First, the measurement of product reducing sugars, specifically glucose, cellobiose and xylose, have been a source of large losses in accuracy. Secondly, the nature of the enzyme assay, i.e. solid-liquid reactions give rise to additional variance in, not only the kinetics of conversion but also the ultimate yield of measureable products. In the first case mentioned above, the use of colorimetric methods for reducing sugar determinations for relative sugar production is one of the major sources of inaccuracy. Problems arise when the results of these methods are published when in fact they are generally erroneous because all reducing substrates are measured with variable extent of sensitivity. For example, in this laboratory, 3,5-dinitrosalicylic acid reagent (1) is used for the colorimetric determination of relative production of reducing sugars. When glucose is used as the standard, values for cellobiose are low by 23% and values for xylose are 15% high on a

weight basis. However, on a molar basis xylose is equal to glucose but cellobiose is low by 33%. With the use of more specific methods, such as silylation of the reducing sugars and determination of the silyl ether derivatives by gas/liquid chromatography, the loss in accuracy has been reduced to less than ±1%. Lately, with the use of high, or even low, pressure liquid chromatography the loss in accuracy is quite low, i.e., less than ±2%. However, these instruments are usually quite expensive, though they amortize themselves relatively quickly with the increased output and accuracy. Glucose specific assays are accurate after they are modified to accommodate the various substrates used and hydrolyzates encountered. The use of glucose oxidase-peroxidase method in automatic glucose analyzers is a great improvement over the laborious manual GOP method. Here again, these instruments are quite expensive.

The second cause mentioned above, the various substrates used, have given rise to an wide array of results. Since the enzyme produced from various organisms is variable in composition, even on a given production run, coupled with the variable substrates used, the results are difficult at best to utilize. It is expected in the near future this problem should be greatly reduced when the somewhat refined methods of direct enzyme composition are established as opposed to the present secondary or indirect methods. Of course, the ultimate utility of any enzyme is its effectiveness under process conditions.

In this laboratory, the present methods for cellulase enzyme characterization are: 1) filter paper activity,

(FPA). 2) (C_x an obsolete term) or endo-β-1,4 glucanase or carboxymethyl cellulase, abbreviated as CMC'ase, since carboxy methyl cellulose is used as the substrate. 3) (C_1, an obsolete term) cellobiohydrolase, abbreviated as CBH or loosely called exo-β-1,4 glucanase. 4) β-glucosidase, also called cellobiase since cellobiose is used as a substrate. 5) soluble protein. The broad measure of these activities are calculated based on product glucose in micromoles (0.180 mg) per minute or 10.8 mg per hour. This is the definition of one International Unit of enzyme activity.

The following is a very brief description of the methods described above. The Filter Paper Activity is based upon the overall action of cellulase enzyme on 50 mg of Whatman #1 filter paper, an easily hydrolyzable substrate, at 50°C for 1 hour. It is not shaken or otherwise mixed after the initial mixing to distribute the filter paper strip uniformly in the diluted enzyme solution. The glucose and cellobiose produced is measured as glucose with DNS reagent. As expected, the precision of this procedure does vary as much as 25%. As a means of tracking enzyme growth this procedure is adequate. However, because of the reasons mentioned previously, it should not be reported as the only means of characterization of cellulase enzyme. To demonstrate how tenuous this test is, the results of filter paper activity measurements comparing the glucose and cellobiose produced, determined by high pressure liquid chromatography (HPLC) with cellulase enzyme derived from Trichoderma reesei QM 9414 are shown in Figures IB-1 and 2,

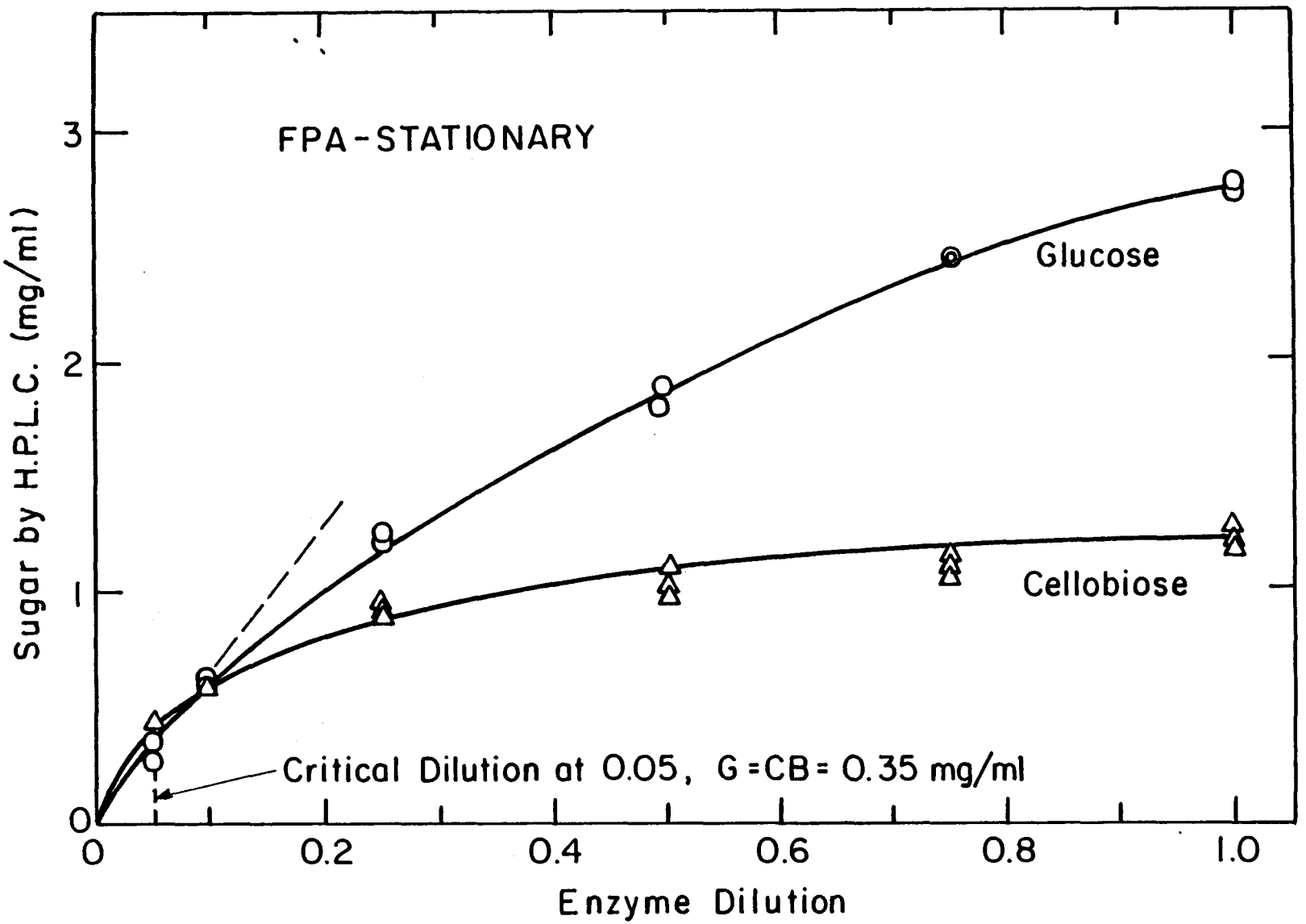

XBL822-5255

Fig. IB-1. FPA Dilution curve of T. reesei (QM9414 cellulase diluted with 0.05M acetate buffer pH5; plus 50 mg (1 x 6 cm) Whatman #1 filter paper mixture stationary at 50°C for 60 minutes, 2 ml total volume.

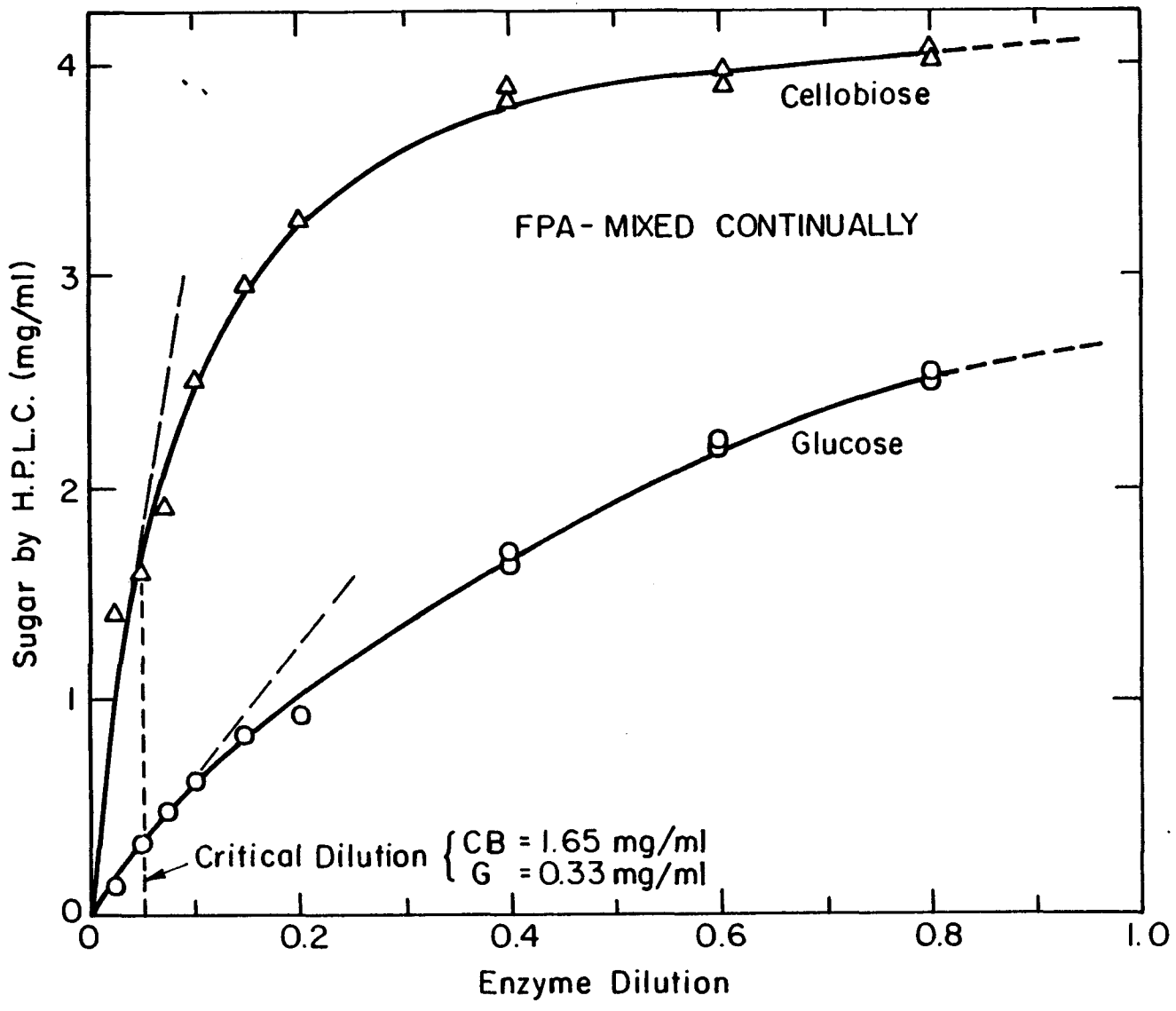

Figure IB-2. FPA Dilution curve of T. reesei QM 9414 cellulase diluted with 0.05M Acetate buffer pH5, plus (1 x 6 cm) Whatman #1 filter paper shaker at 200 cycles/min., at 50°C for 60 minutes, 2 ml total volume.

respectively. In Figure IB-1, the results from a static (i.e. not continually mixed) FPA enzyme dilution run are plotted to determine the critical dilution, defined as the onset of non linearity of enzyme activity, for this particular type of test. In this case the critical dilution was 0.05 concentration of initial enzyme. The glucose Filter Paper Activity was 1.3 IU(G) per ml, and the cellobiose was 0.65 IU(CB) per ml. In Figure IB-2, the results of a similar enzyme dilution run is shown except each of the enzyme activity assays were shaken at 200 cycles per minute for the 60 minutes. As shown, at critical dilution, there is about the same activity for glucose produced of 1.2 IU(G) per ml, however, there is a considerable increase in cellobiose activity of 3.4 IU(CB) per ml. To complicate the matter further, in the previous shaker run, the DNS colorimetric method for "reducing substances" was used to determine the product versus a glucose standard. The results of this enzyme dilution curve are shown in Figure IB-3. As shown, at critical dilution of 0.05, the FPA of 2.1 IU/ml was obtained. This value is an apparent average compared to previous run (Fig. IB-2). This is soley due to an artifact of the concentration ratios of the cellobiose and glucose along with product inhibition of cellobiose as is also shown in Figure IB-2. These examples are shown to demonstrate part of problems encountered with published results. With cellulase enzyme solution derived from T. reesei Rut C-30 containing considerably higher concentration of β-glucosidase, the effects of cellobiose are proportionately reduced. The typical FPA assays performed now produce less than

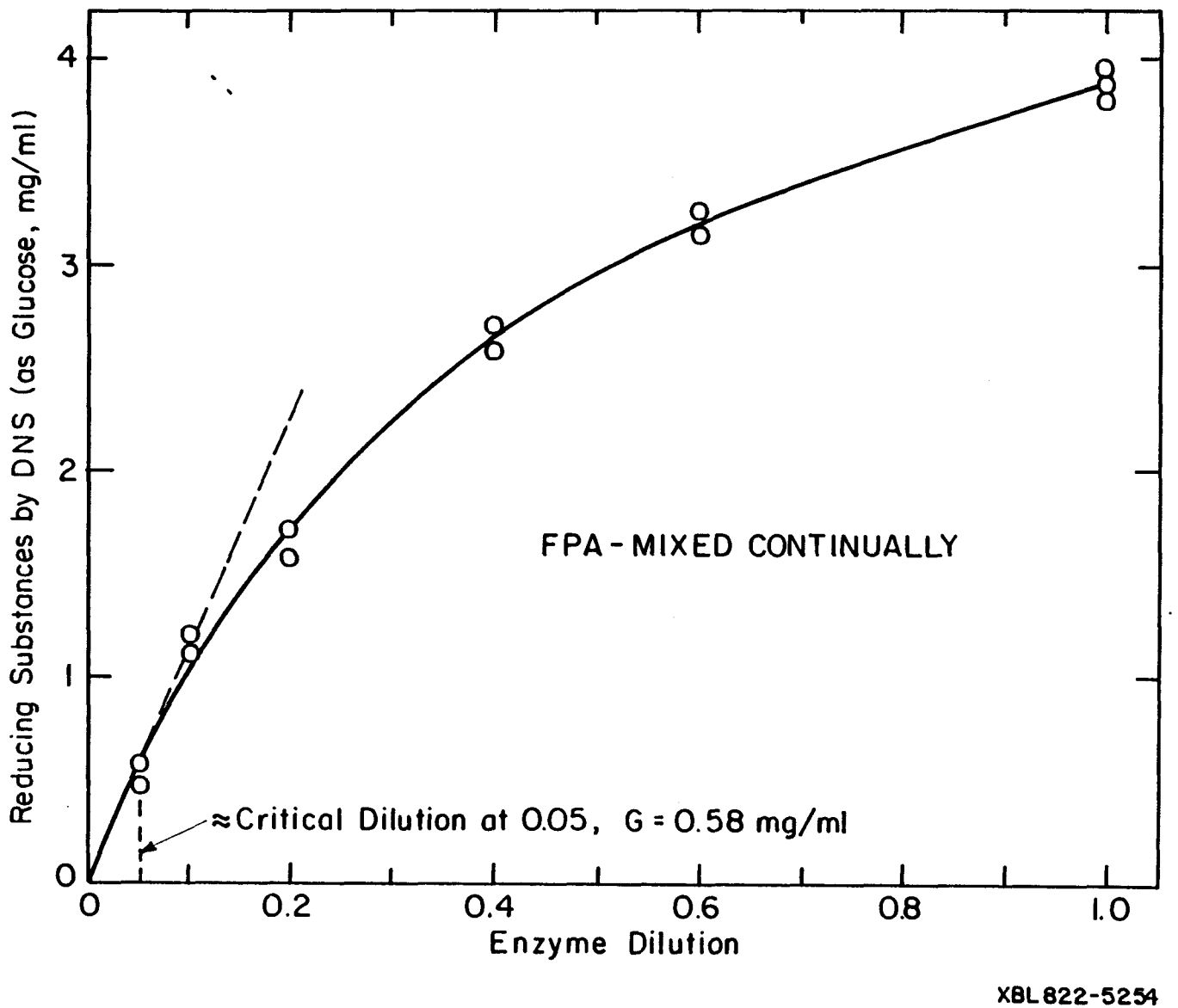

Fig. IB-3. F.P.A. dilution curve of T. reesei QM9414 cellulase diluted with 0.5 M acetate buffer pH5, plus 50 mg (1x 6 cm) Whatman #1 filter paper shaker at 200 cycles/ min., at 50°C for 60 minutes, 2 ml total volume.

one percent cellobiose of total sugar produced and the determination with DNS reagent is usually adequate. The results of a typical FPA enzyme dilution curve is shown in Figure 1B-4. The original enzyme was diluted 1:10 (x 11) prior to this determination and at a further relative dilution of 0.3 the sugar produced as glucose=0.544 mg/ml. An example of the calculation of FPA in terms of I.U. is thus:

FP = (0.544mg G/ml)(2 ml)(1/0.3 x 1ml)(0.0926)(x 11) = 3.7 I.U./ml.

The determination of endo-β-1,4 glucanase (CMC-ase) is performed with carboxymethyl cellulose as substrate and is specified as CMC-7L (Hercules) DP-400, DS = 0.65-0.85. One ml of a 2wt% solution of the CMC in 0.025 M acetate buffer, pH = 5, is used along with 0.1 ml of the diluted enzyme, mixed and then maintained at 50°C for 30 minutes. The reaction is quenched with DNS reagent and the product sugar, as glucose, is measured. The result of the relative enzyme dilution curve with the same enzyme solution used for previously described FPA is shown in Fig. IB-5. The original enzyme was diluted 1:20 (x21) prior to this determination. An example of the calculation of the activity is thus: CMC-ase= (0.490 mg G/ml)(1.1ml)(1/0.21 x 0.1ml)(0.1852)(x 21) = 100 I.U./ml.

The determination of cellobiohydrolase (CBH) is performed with cotton as the substrate and is specified as Johnson and Johnson (Red Cross) brand. 1 ml of the diluted

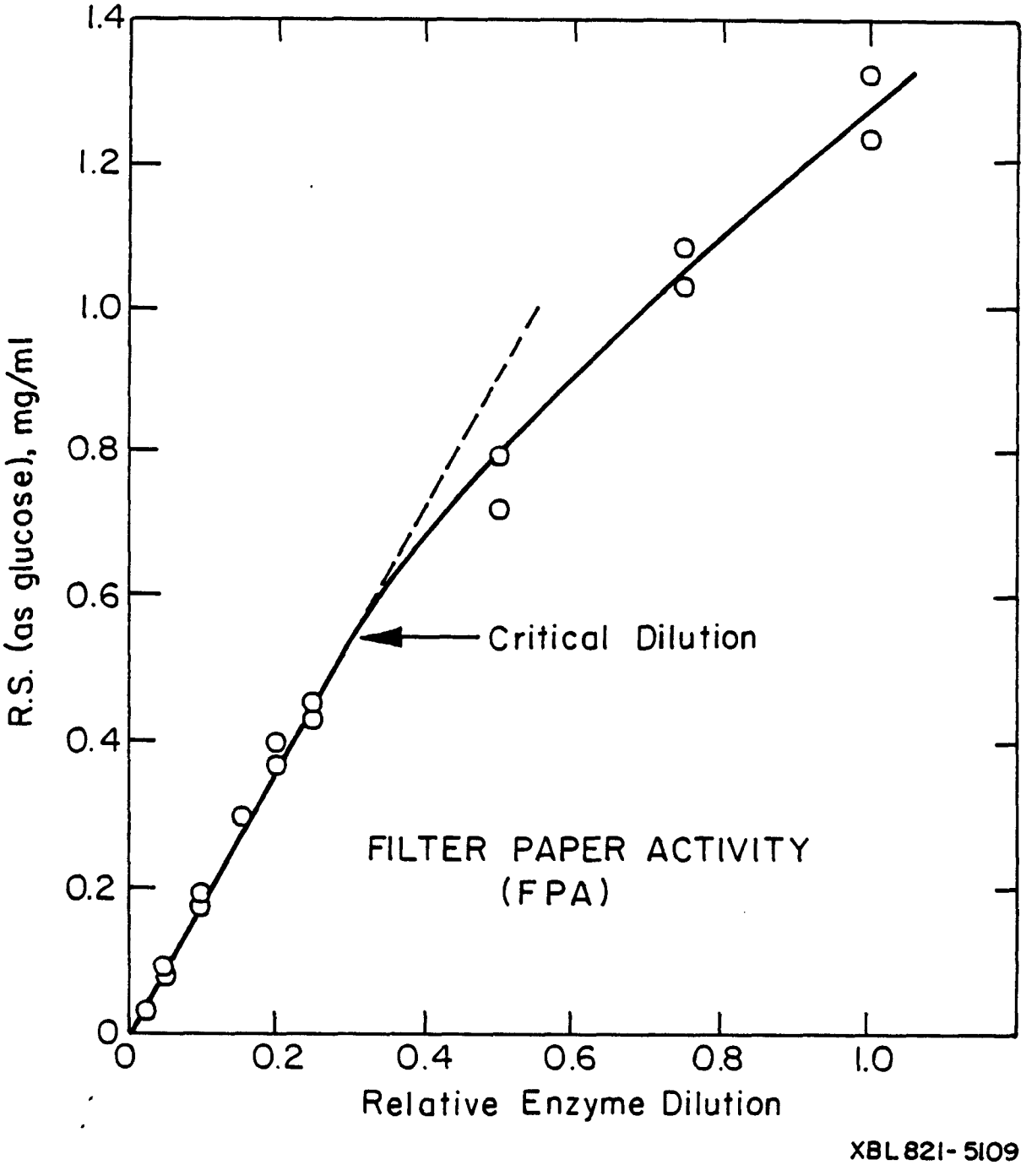

Figure IB-4. FPA dilution curve of T. reesei cellulase enzyme Rut-C30 diluted with 0.025 M acetate fuffer, pH5. 1.0 ml diluted enzyme plus 1 ml buffer plus (1 x 6 cm) Whatman #1 Filter Paper, stationary at 50°C for 60 min. Assayed with DNS.

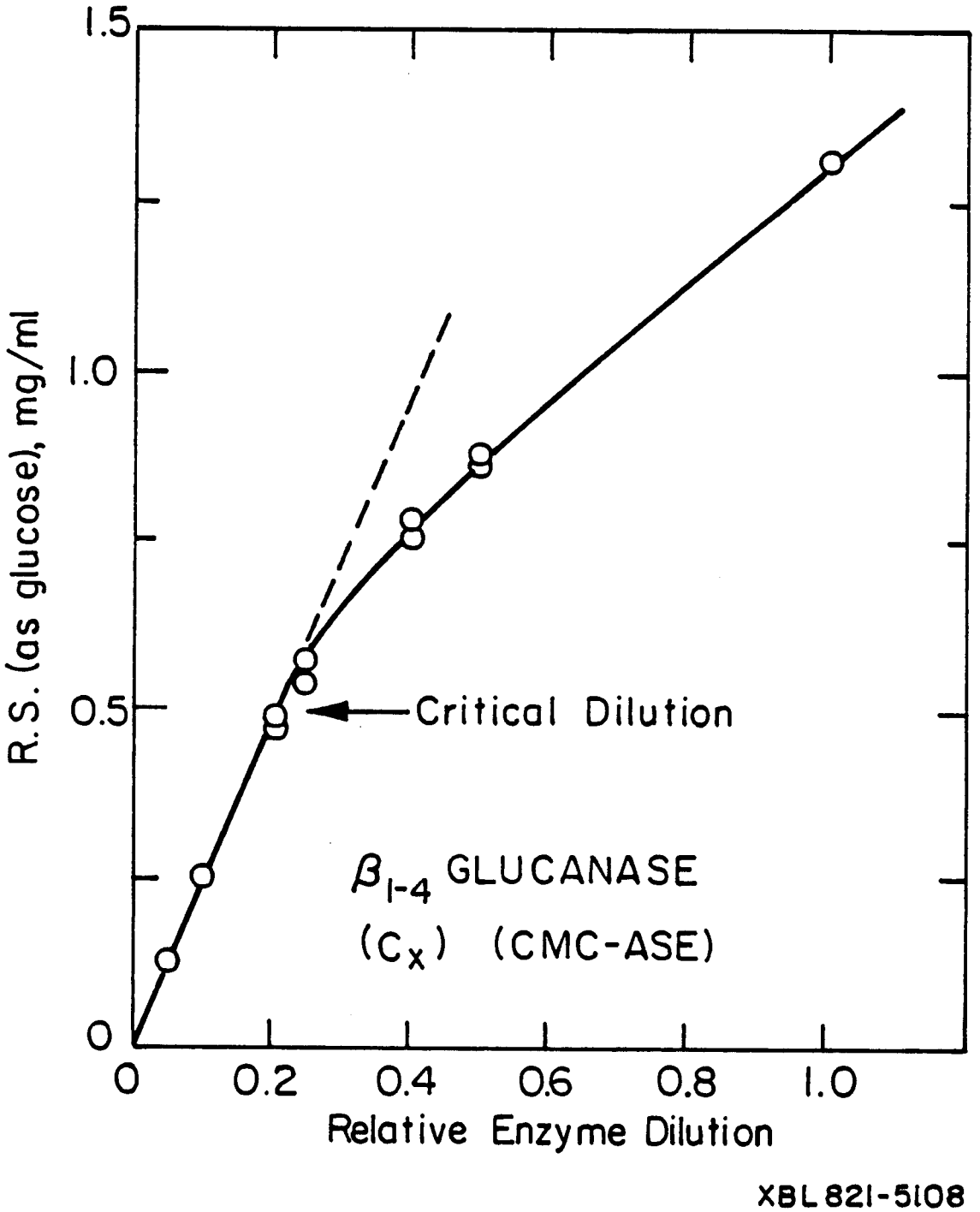

Figure 1B-5. CMC-ase Dilution Curve of T. reesei Cellulase Enzyme Rut C-30 Diluted with 0.025 M Acetate Buffer, pH5. 0.1 ml Diluted Enzyme Plus 1.0 ml 2% CMC, Stationary at 50°C for 30 Minutes. Assayed with DNS.

enzyme and 1 ml of 0.05 M acetate buffer, pH = 5, is mixed with 50 mg of the above cotton and allowed to stand at 50°C for 24 hours. The reaction is then quenched with DNS and the product sugar, as glucose, is measured. The result of the relative enzyme dilution curve with the previous example enzyme solution is shown in Figure IB-6. The original enzyme solution was diluted 1:20 (x21) prior to this run. Since this run is performed for 24 hours the factor for IU = 1/(0.18 mg x 24 x 60) = 3.858×10^{-3} I.U./mg G. An example of the calculation of this activity is thus:

$$\text{CBH} = (0.36\text{mg G/ml})(2\text{ ml})(1/0.42 \times 1\text{ ml})\ (3.858 \times 10^{-3})(\text{x21})$$
$$= 0.14\text{ I.U./ml.}$$

The determination of β-glucosidase (CB-ase) is performed with cellobiose as the substrate and is specified as J.T. Baker Chem. Co. #E-403 (Baker Grade), because of considerable variability of purity encountered with that which is commercially available. 0.1 ml of the dilute enzyme is mixed with 1 ml of 1.25% cellobiose in 0.025 M acetate buffer, pH = 5, and allowed to react at 50°C or 30 minutes. The reaction is quenched with glucose oxidase-peroxidase reagent (2) that is modified with tris (hydroxymethyl-amino methane) buffer, pH = 7, (3). Alternatively, the reaction can be quenched, with 0.025 ml of concentrated hydrochloric acid when the glucose anayzer is used. The result of the relative enzyme dilution curve with the previous example enzyme is shown in Figure IB-7. Not shown in

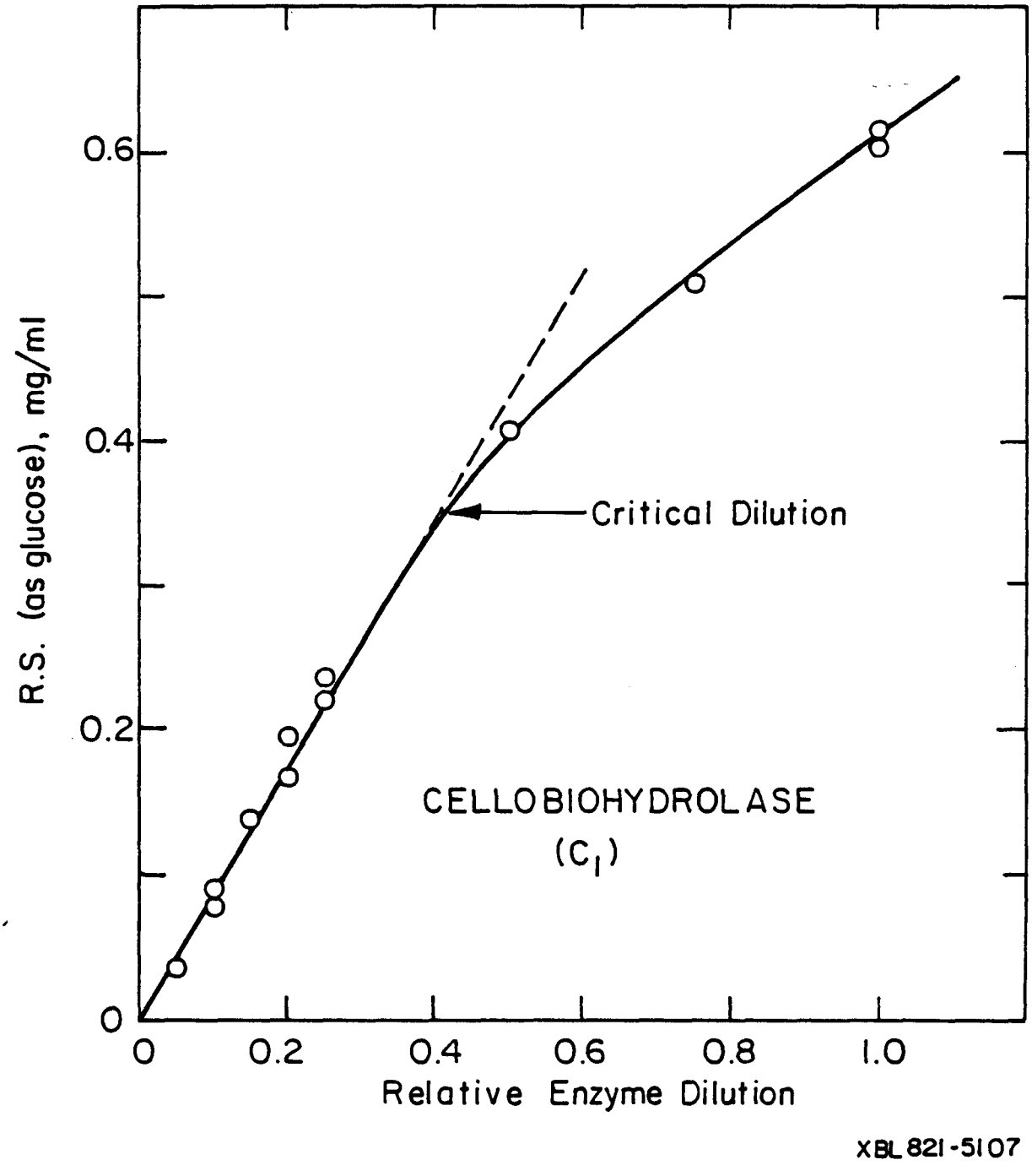

Figure IB-6. CBH Dilution Curve of T. reesei, Cellulase Enzyme Rut-C30, Diluted with 0.025 M Acetate buffer, pH5. 1.0 ml Diluted Enzyme plus 1 ml Buffer plus 50 mg Red Cross Cotton, Stationary at 50°C for 24 hours. Assayed with DNS.

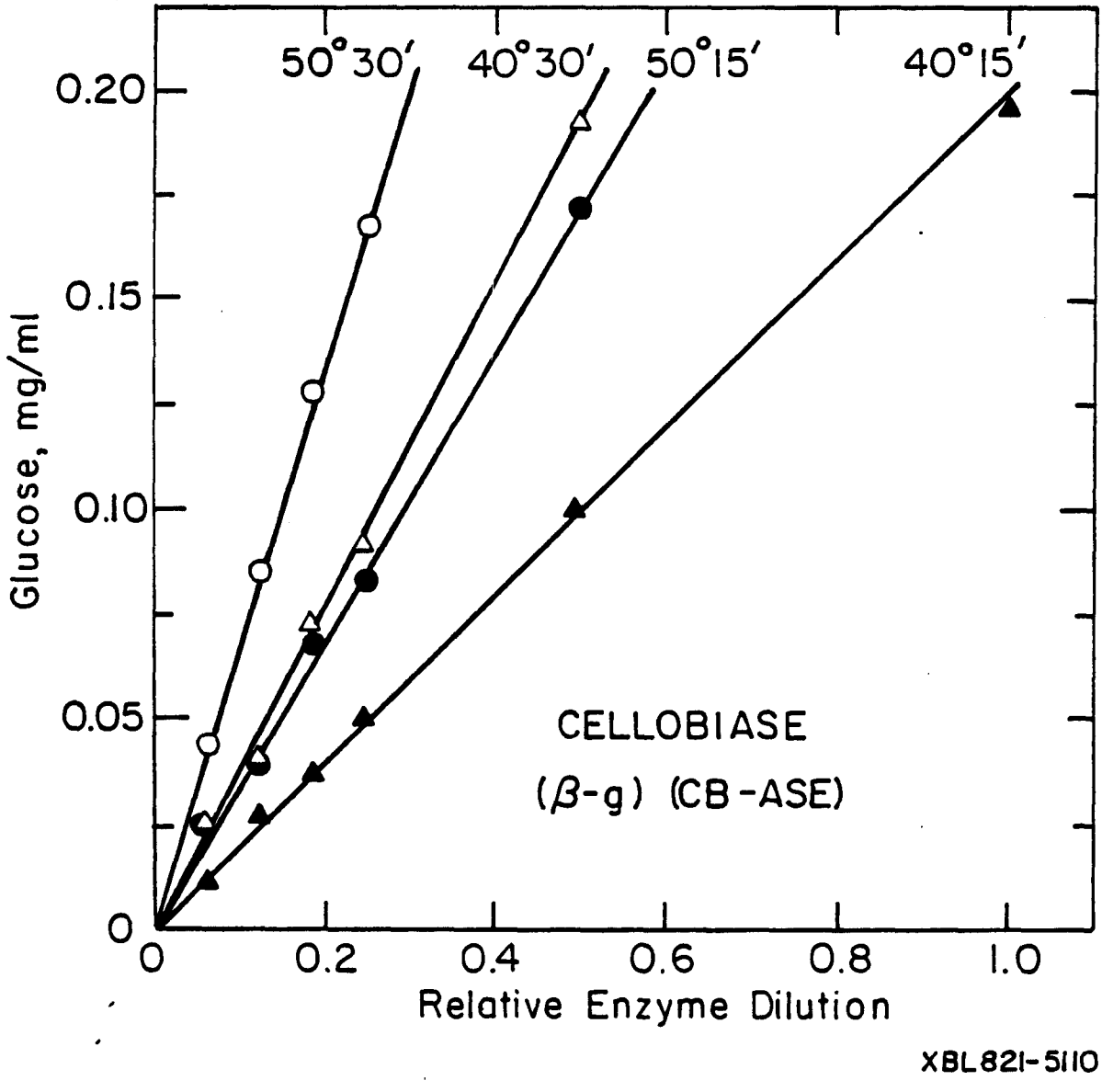

Figure IB-7. Cellobiase Dilution Curve of T. reesei Cellulase Enzyme Rut-C30, Diluted with 0.025 M Acetate Buffer, pH5. 0.1 ml Diluted Enzyme Plus 1.0 ml 1.25% Cellobiose, Stationary at Indicated Temperatures and Times. Assayed with GOP.

Figure IB-7, the critical diluton for 30 minutes at 50°C is 0.66 mg G/ml at 1.0 relative enzyme dilution. The original emzyme solution was diluted 1:3 (x4) prior to the run. An example of the calculation of the activity is thus:

$$B\text{-}g = (0.16 \text{ mg G/ml})(1.1 \text{ ml})(1/0.24 \times 0.1 \text{ ml})(0.1852)\ (x4)$$
$$= 5.4 \text{ I.U./ml.}$$

In Figure IB-7 is also shown the linearities of other reaction times and temperatures. The necessity of careful control of temperature and reaction times are indicated by these results.

The soluble protein is measured by the method of Lowry, et al. (4) and with Rutger C-30 cellulase enzyme, values of 6 to 7 mg/ml are encountered.

3. Future research

The Biotechnology Commission of IUPAC has asked the group at the US Army Natick RD Labs to coordinate the preliminary concensus procedures. In addition they have supplied the necessary freeze dried enzymes, substrates and reagents for the collaborative study. These procedures, some of which we are familiar with, should present very little problems. Others appear to be difficult and tedious, and that may preclude their uility. The principle for enzyme evaluation under process conditions appears to be well suited and most necessary at this time. The procedure is in a state of flux but this study should resolve some of the questions.

References

1. Miller, G.L., Anal. Chem., 31#3, 426 (1959).

2. Morin, L.G., J. Prox, Clin Chem, 19#9, 959 (1973).

3. Riaz, M., "Cellulolysis by Enzymic Components of Cellulolytic Fungi with Particular Reference to Myrothecium Versucasia and Trichoderma koningii, Ph.D. thesis, Univ. of Wales, U.K. (1964)pp.96 -101.

4. Lowry, O.H., N.J. Rosebrough, A.L. Farr, R.J. Randall, J. Biol. Chem., 193, 265 (1951).

II. FUNDAMENTAL STUDIES OF HIGH PRODUCTIVITY FERMENTATIONS

A. Basic Studies on Yeast Nutrition

1. Introduction

A basic study of the nutrient requirements for yeast fermentation of sugars to ethanol is important because of the high cost contribution of the nutrients to the ethanol production cost and because of the major effects of medium composition on ethanol and yeast productivities. In all known ethanol producing processes, the growth factors and many of the minerals are provided from complex sources such as molasses or cornsteep liquor. Up to now there has been little effort devoted to defining the active components of these complex sources in yeast fermentation and to defining their optimal ratios for a balanced medium. A balanced medium is important to eliminate the cost of excess components and to prevent their inhibitory effects on build-up in recycle processes with selective ethanol removal. Therefore, batch and continuous fermentations are being carried out with synthetic and semisynthetic media to define quantitatively the usage of all the major media components for cell growth and ethanol production.

2. Current Research

a. Nutrient studies under low glucose, low ethanol conditions.

After the important growth factors were identified in batch fermentation, continuous cultures were started to determine the optimum levels of all the medium components in ethanol fermentation. The first case considered

was a medium with only 10-15 g/L glucose to eliminate the effects of ethanol inhibition and glucose inhibition on the medium requirements.

i) Procedures

A novel procedure extending developments by Mateles and Battat (1) was employed. Each medium component is made the limiting substrate in terms of cell and ethanol yields. The limiting nutrient is first determined by observing which component when injected as a concentrated pulse directly into the fermenter produces a transient increase in cell mass or ethanol. The yields of cell mass and ethanol with respect to the limiting nutrient can then be determined from the known steady state feed rate of the limiting nutrient and known productivity rates of cell mass and ethanol prior to the injection. When this limiting nutrient is found, its concentration in the feed reservoir, which is feeding at a steady state dilution rate, is increased such that it is no longer yield limiting up to a given level of cell mass and ethanol. This component can then be eliminated from further testing as the other components in turn are each made yield limiting.

In Table IIA-1 is given the minimal medium and the concentrations of the vitamins tested. The concentrations given for biotin, pantothenic acid, pyridoxine, and thiamine are for the feed bottle after positive responses were seen for their pulse injections into the fermentor. The concentrations given for inositol, nicotinic acid, and p-aminobenzoic acid are for the fermentor upon injection if not consumed. Note there is a very

Table IIA-1

Standard Minimal Medium

	g/L
$(NH_4)_2SO_4$	0.472
KCl	0.0763
$Ca_2Cl_2 \cdot 2H_2O$	0.0118
$MgSO_4 \cdot 7H_2O$	0.0495
Yeast Extract	0.100
H_3PO_4	0.084
Trace Minerals Solution	0.5 ml/L

Trace Minerals Solution

	g/L
H_3BO_3	3.0
$CoSO_4 \cdot 7H_2O$	0.2
$CuSO_4 \cdot 5H_2O$	0.8
$ZnSO_4 \cdot 7H_20$	2.0
$MnSO_4 \cdot H_2O$	0.6
KI	0.2
$FeSO_4 \cdot 7H_2O$	0.4
$Al_2(SO_4)_3$	0.6

Vitamin Additions (only when specified)

Biotin	4µg/L
Pantothenic Acid	1.25 mg/L
Pyridoxine	1.25 mg/L
Thiamine	0.133 mg/L
Inositol	3.45 mg/L
Nicotinic Acid	1.12 mg/L
p-Aminobenzoic Acid	0.0518 mg/L

small quantity of yeast extract (0.1 g/L) present to provide for the possible trace requirements which cannot presently be determined. This allows determination of all the major components in the meantime.

ii) Results and Discussion

The positive responses to pulse injections of nutrients are given in Table IIA-2, which shows the steady state fermentor conditions before injection and the transient conditions after the specified times. The minimal medium composition and the unspecified component concentrations referred to in this table are those given in Table IIA-1. The cell optical densities (O.D) can be converted to dry weight concentrations with the calibration in Figure IIA-1.

The minimal medium without any vitamins added showed low cell and ethanol productivities with only about one third of the available glucose consumed. Biotin added to this medium as a pulse gave a very positive response. The steady state response of biotin in the feed showed that the cell and ethanol productivities increased by about three times.

Pantothenic acid was the next growth factor to show a positive pulse response after the biotin requirement was met. In fact, previous studies showed that unless this biotin requirement was first met, pantothenic acid and pyridoxine did not show positive responses, implying biotin is needed for a critical reaction before pantothenic acid or pyridoxine could be utilized in subsequent reactions. The addition of pantothenic acid to the feed medium increased ethanol and cell production to

Table IIA-2

Positive Pulse Response

MEDIA Before Injection	INJECTIONS	ΔTIME (hr)	O.D.	Glucose Consumed (g/L)	EtOH Produced (g/L)
1 x minimal 10g Glucose/L	–	–	0.248	3.69	1.13
–	Biotin (4μg/L) (Feed Bottle)	21.5	0.460	6.79	2.43
1 x(minimal + Biotin) 10g G/L	–	–	0.690	9.03	3.28
–	Pantothenate (2.5 mg/L) (Fermentor)	4.0	0.830	9.42	4.04
1 x (minimal + Biotin + Panto) 15g G/L	–	–	0.915	9.33	3.78
–	Pyridoxine (1.25 mg/L) (Feed Bottle)	13.75	1.030	11.0	4.19
1 x (minimal + Biotin +Panto. + Pyr) 15g G/L	–	–	0.990	12.1	4.28
–	Thia (0.133 mg/L) Inos. (3.45 mg/L) Nico (1.12 mg/L) p-ABA (0.0518mg/L) (Fermentor)	6.75	1.060	13.9	4.73
1 x(minimal + Bio +Panto. + Pyr) 15g G/L	–	–	1.020	12.3	4.49
–	Thia (0.266mg/L) (Fermentor)	7.25	1.035	12.2	4.91
1 x(minimal + Bio + Panto + Pyr + Thia) 15g G/L	–	–	0.990	12.1	4.39
–	Yeast Extract (5 ml of 20 g/L sol'n)(Fermentor)	5.0	1.075	13.1	4.79

Table IIA-2
Continued

Positive Pulse Response

MEDIA Before Injection	INJECTION	Δtime (hr)	O.D.	Gluc. Consumed (g/L)	EtOH Produced (g/L)
2/3 x (minimal + Bio + Panto + Pyr + Thia) 10g G/L	-		0.699	8.69	3.51
-	Mineral Solution (2 x of minimal) (Fermentor)	6.0	0.807	10.2	3.80
2/3 x minimal + Bio +Panto + Pyr + Thi 10g G/L	-	-	0.705	8.90	3.41
-	$(NH_4)_2SO_4$ (4 ml of 250 g/L sol'n (Fermentor)	10.75	0.825	9.81	3.39
1 x $(NH_4)_2SO_4$ 2/3 x Others	-	-	0.972	0.98	3.65
-	KCL Decrease from 2/3 x to 1/3 x (Feed Bottle	36.0	0.813	0.84	3.77

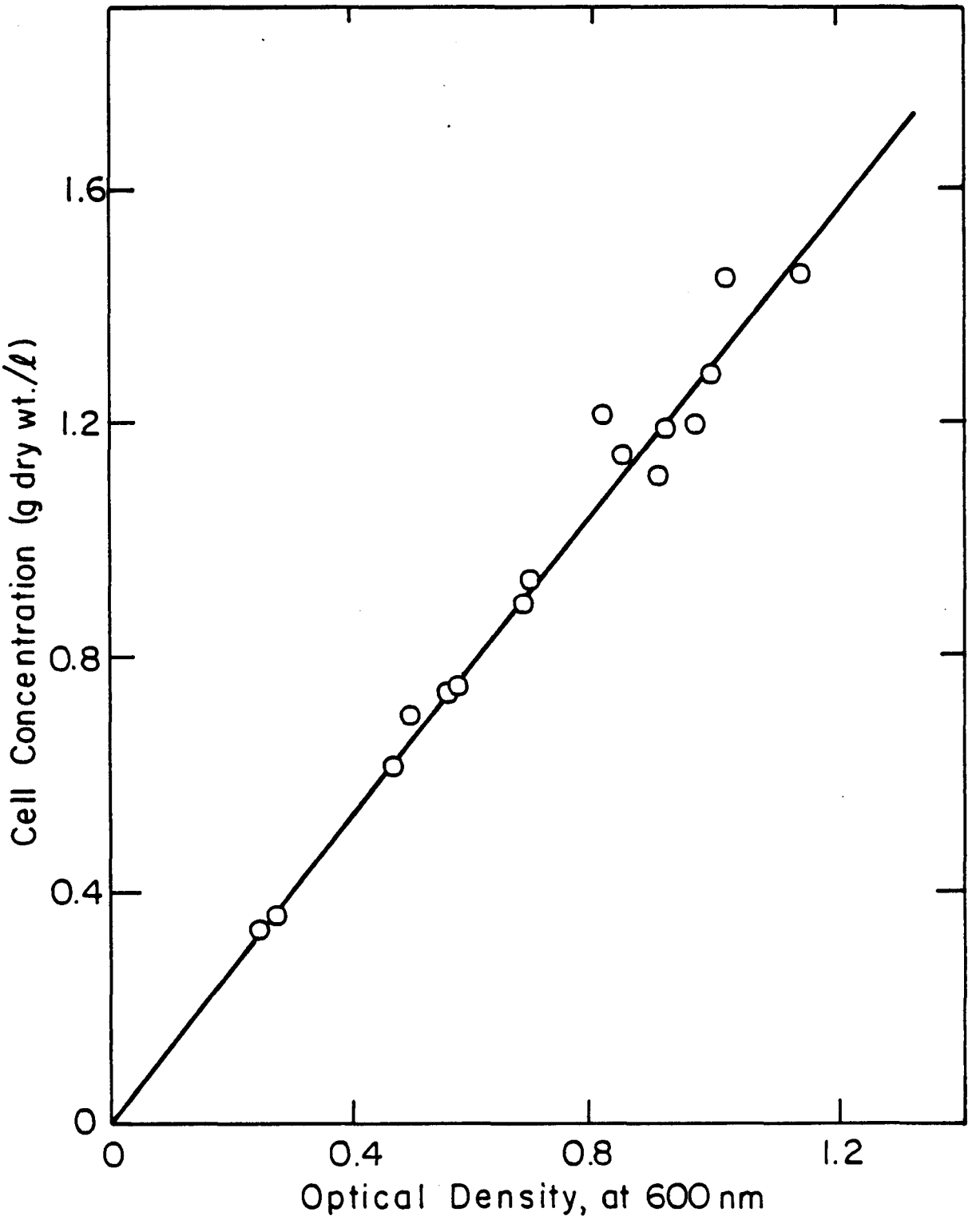

Figure IIA-1. Dry cell mass calibration curve.

the point where the glucose was almost entirely consumed so it then became the limiting substrate. The glucose concentration was then increased to 15 g/L for the steady state pantothenic acid response and for the next growth limiting substrate, pyridoxine.

Pyridoxine gave positive pulse and steady state responses. Next a combination of thiamine, inositol, nicotinic acid, and p-aminobenzoic acid was pulsed into the fermentor with a positive response. After steady state was re-established, thiamine was pulsed with a positive response. However, the steady state response to thiamine addition to the feed showed no significant change. Subsequent injections of inositol, nicotinic acid and p-aminobenzoic acid to the fermentor also showed no response. Yeast extract then gave a positive pulse response, indicating there were still nutrient limitations.

To see the growth limiting concentrations for the medium minerals, the medium was diluted to give 10 g/L glucose and only 2/3 the previous minimal and growth factor concentrations for this glucose level. An injection of a mineral mixture gave a positive response. A subsequent injecion of $(NH_4)_2SO_4$ also gave a positive response, indicating it was the limiting component that was responsible for the earlier positive response. The steady state response for $(NH_4)_2SO_4$ addition to the feed showed a significant cell increase but a smaller ethanol increase.

The steady state continuous culture responses to medium composition shifts are given in Table IIA-3. The

Table IIA-3

Steady-State Glucose, Cell Mass and Ethanol Data

MEDIA	Dilution	Glucose (g/L)		Dry Cell Mass		Ethanol		
	Rate (hr^{-1})	Feed	Utilized	g/L	$Y_{x/s}$	g/L	$Y_{p/s}$	q_p
(1 x) minimal	0.27	10.1	3.66	0.322	0.0880	1.13	0.309	0.948
(1 x)(minimal + Biotin)	0.27	9.84	9.03	0.897	0.00993	3.28	0.363	0.987
(1 x)(minimal + Biotin + Pantothenic Acid)	0.27	9.84	9.62	1.20	0.125	4.37	0.454	0.983
(1 x) Minimal+ Biotin +Pantothenic Acid)	0.345	9.89	6.20	0.751	0.121	2.12	0.342	0.974
(1x)(Minimal + Biotin +Pantothenic Acid)	0.42	10.0	2.86	0.348	0.122	1.44	0.503	1.74
(1 x) (Minimal + Biotin +Pantothenic Acid)	0.27	14.2	8.79	1.19	0.135	3.78	0.430	0.858
(1 x)(minimal + Biotin + Pantothenic Acid +Pyridoxine)	0.27	14.9	12.1	1.29	0.107	4.28	0.354	0.896
(1 x)(minimal +Biotin + Pantothenic Acid + Pyridoxine + Thiamine)	0.27	14.9	12.8	1.48	0.116	4.69	0.366	0.856
(2/3 x)(minimal + Biotin + Pantothenic Acid + Pyridoxine + Thiamine)	0.27	10.24	8.69	0.909	0.105	3.51	0.404	1.04
Same	0.27	10.24	8.82	0.909	0.103	3.54	0.401	1.05
(1 x) $(NH_4)_2SO_4$, (2/3 x) (Other minerals + Biotin + Pantothenic Acid + Pyridoxine + Thiamine)	0.27	10.0	9.75	1.26	0.129	3.65	0.374	0.782

$Y_{x/s}$ = g cell/g glucose consumed
$Y_{p/s}$ = g ethanol/g glucose consumed
q_p = g ethanol/g cells/hr

incremental effects of adding biotin, pantothenate, pyridoxine, thiamine and ammonium sulfate can be determined from this table. The effects of varying dilution rates for the biotin and pantothenate supplemented medium are also presented. The highest ethanol yield, 0.503 g ethanol/g glucose consumed, and the highest specific ethanol productivity, 1.74 g ethanol/g cell/hr, occurred with biotin and pantothenic additions at 0.42 hr^{-1} dlution rate. The highest specific productivity is consistent with the highest dilution rate utilized. However, the ethanol yield corresponds to the theoretical maximum from glucose if no cell mass is produced and if the yeast extract is disregarded. Thus, there is some doubt about the accuracy of either the glucose or ethanol measurements for this particular case. The next highest yield was 0.454 g ethanol/g glucose utilized and was obtained with the same biotin and pantothenate supplements at 0.27 hr^{-1} dilution rate. The next highest specific ethanol productivity was 1.05g EtOH/g cell/hr obtained with biotin, pantothenate, pyridoxine, and thiamine additions to the mimimal medium.

With a recycle process which can produce high cell densities, high specific ethanol productivity will result in high total productivity. However, the cost of ethanol production will be largely determined by its yield with respect to its sugar substrate. Therefore, sugar should be made the limiting substrate. To make sugar limiting, the usage or inversely the yield of ethanol with respect to all other medium components must be known so they will not become limiting. Based

on the yields obtained when each was made the above limiting substrate in the experiments, the yield coefficients given in Table IIA-4 can serve as approximate guidelines for scale-up to higher concentration systems.

3. Future Research

Future work will be directed at scale-up of the low glucose, low ethanol conditions to higher glucose (100 g/L) and correspondingly higher ethanol. As a basis for comparison, yeast extract as a general nutrient source will be studied at varying concentrations. Then the effects of varying individual mineral and vitamin concentrations in a highly synthetic medium will be determined. The feasibility of both a completely synthetic medium and a semisynthetic medium with an inexpensive complex component, for example, cornsteep liquor will also be investigated. Finally, having determined the usage requirement of each medium component from synthetic or highly synthetic medium studies and knowing the composition of the inexpensive complex component of the medium as well as knowing all costs, the optimum blend of components for the medium will be determined with a linear program. This program can be used to give the economicaly optimum medium as prices change for various components.

References

1. Mateles, R.J., E. Battat, Applied Microbiology, 28(6) 901-905 (1974).

Table IIA-4

Yield Coefficients

MEDIA	LIMITING COMPONENT	g.dry cell per g limit comp.	g G used/ g limit comp	g EtOH Produced/ g limit comp.
(1x)(minimal) 10g Glucose/L	Biotin	3.22×10^6	3.69×10^7	1.13×10^7
(1x)(minimal + Biotin) 10g G/L	Panthothenate	8.97×10^4	9.03×10^5	3.28×10^5
(1x)(minimal + Bio+Pant) G/L	Pyridoxine	5.95×10^5	4.67×10^6	1.89×10^6
(1x)(minimal+Bio+Pant+Pyr) 15g G/L	Thiamine	4.42×10^6	4.10×10^7	1.50×10^7
(1x)(minimal+Bio+Pant +Pyr+Thia) 15g G/L	$(NH_4)_2SO_4$	3.14	27.1	9.94
(2/3x)(minimal+Bio+Pant +Pyr+Thia) 10g G/L	$(NH_4)_2SO_4$	2.89	27.6	10.7
(1x)$(NH_4)_2$ SO_4 2/3 x others 1/3 x KCl 10g G/L	KCl	1.4	388	147

B. Models of Yeast Growth and Ethanol Production

Oxygen Uptake under Fermentation Conditions

1. Introduction

Under aerobic conditions the yeast demand for oxygen can be determined from the overall reaction for aerobic growth given by Harrison (1):

$$\underset{100.00\ g}{0.55556\ C_6H_{12}O_6} + \underset{5.10\ g}{0.30017\ NH_3} + \underset{46.63\ g}{1.45729\ O_2} \rightarrow \underset{43.23\ g}{0.30017\ C_6H_{10}O_3N} + \underset{41.08\ g}{2.28276\ H_2O} + \underset{67.42\ g}{1.53234\ CO_2}$$

Most all of the oxygen consumed by the above reaction goes into the catabolic function of respiration as the terminal electron acceptors in oxidative phosphorylation. This use of oxygen for respiration is well understood and large enough such that it can be easily measured.

However, oxygen is also required for less well understood biosynthesis under both aerobic and fermentative conditions. It has been shown repeatedly that complete anaerobiosis results in very low cell and ethanol productivity (Haukeli and Lie (2), Cysewski and Wilke (3)). Moreover, adding both ergosterol and unsaturated fatty acids to the medium gave relatively high cell yields even under anaerobiosis (Andreasen and Stier (4)). This suggests that oxygen is required for the synthesis of ergosterol and unsaturated fatty acids. Both of these are important components of yeast lipid, the bulk of which is required for cell membranes. However, the biosynthesis requirement for oxygen is very low and difficult to measure. It is even ignored by Harrison (1) in his overall reaction for

fermentation:

$$0{\cdot}55556\ C_6H_{12}O_6 + 0{\cdot}01214\ NH_3 \rightarrow 0{\cdot}01214\ C_6H_{10}O_3N + 0{\cdot}05697\ C_3H_8O_3$$
$$100{\cdot}00\ g \qquad 0{\cdot}21\ g \qquad 1{\cdot}748\ g \qquad 5{\cdot}241\ g$$
$$+ 0{\cdot}01204\ C_4H_6O_4 + 0{\cdot}00071\ C_4H_{10}O + 0{\cdot}01164\ H_2O + 1{\cdot}03076\ CO_2$$
$$1{\cdot}42\ g \qquad 0{\cdot}05\ g \qquad 0{\cdot}21\ g \qquad 45{\cdot}32\ g$$
$$+ 1{\cdot}00380\ C_2H_6O$$
$$46{\cdot}17\ g.$$

The objective of this research is to determine the fermentative oxygen requirement and its relationship to cell and ethanol productivities.

2. Procedure

All yeast fermentations are linear combinations of Harrison's two above approximate reactions. Thus it is possible to calculate the fermentative oxygen demand by measuring the total oxygen uptake and subtracting out the oxygen uptake from aerobic growth. The relative extents of aerobic growth to fermentation can be determined from the respiratory quotient, which is the ratio of the carbon dioxide evolution rate to the oxygen consumption rate.

Using a continuous culture, the carbon dioxide evolution rate was determined by measuring the total gas outlet rate from the fermentor and by measuring its CO_2 composition by gas chromatography. The oxygen consumption rate was measured by the dynamic method described by Taguchi and Humphrey (5). This method requires measuring the dissolved oxygen concentation (D.O.) in the fermentor as a function of time with a dissolved oxygen probe. After a steady state D.O. is reached, the gas

inlet containing the O_2 source is turned off. The slope of the D.O. decline gives the O_2 consumption rate. A typical trace is shown in Figure IIB-1. The initial steady D.O. level is varied by changing the agitation rate.

The yeast metabolism is assumed to be still predominantly fermentative even when the D.O. is raised mainly because of glucose repression of respiration and because of the short time exposure to the higher D.O. level in some cases. According to Suomalainen, Nurminen, and Oura (6), glucose concentrations over 50-100 mg/L result in mainly or partly fermentative metabolism even with intense aeration. Ferdouse, Rickard, Moos and Blanch (7) observed that mitochondria and aerobic cytochromes appeared in yeast between three to six hours after the transition from anaerobiosis to 3 M dissolved oxygen in the presence of only 0.02 to 1.66 mM glucose.

3. Results and Discussion

The specific oxygen consumption q_{O2} as a function of the initial dissolved oxygen level are plotted in Figures IIB-2,3,4,5,6,7 and 8 for dilution rates (hr^{-1}) of 0.067, 0.091, 0.151, 0.207, 0.254, 0.313 and 0.397, respectively. For each dilution rate q_{O2} rises rapidly with respect to dissolved oxygen up to a critical concentration. Above this concentration q_{O2} rises slowly up to a plateau called q_{O2} max. These q_{O2} max values are then plotted against dilution rate in Figure IIB-9. Note that for 0.067 hr^{-1} dilution rate in Figure IIB-2, q_{O2} does not reach a plateau for q_{O2} max and so does not appear in Figure IIB-4.

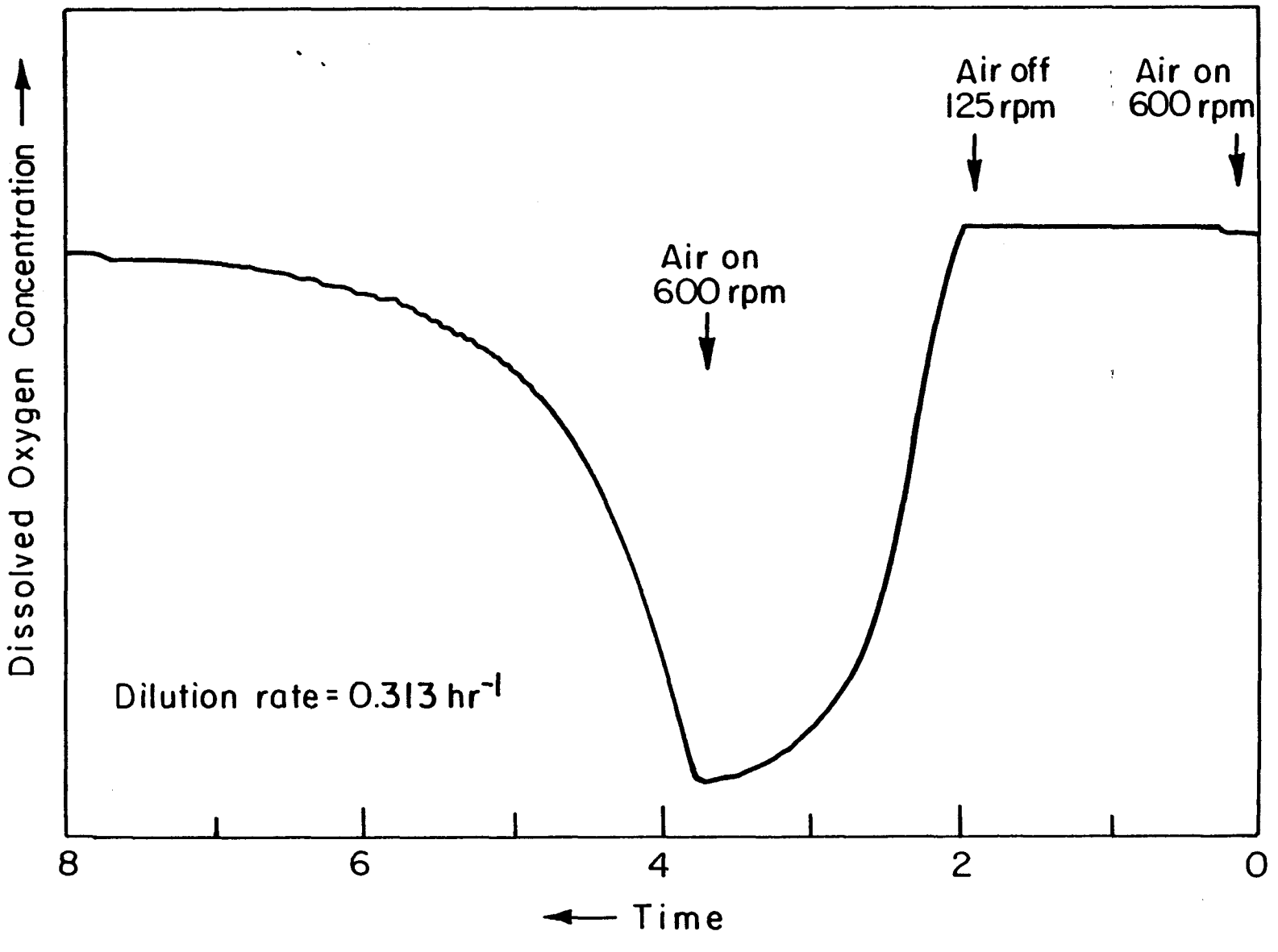

Figure IIB-1 Typical dissolved oxygen trace for q_{O_2} and $K_L a$.

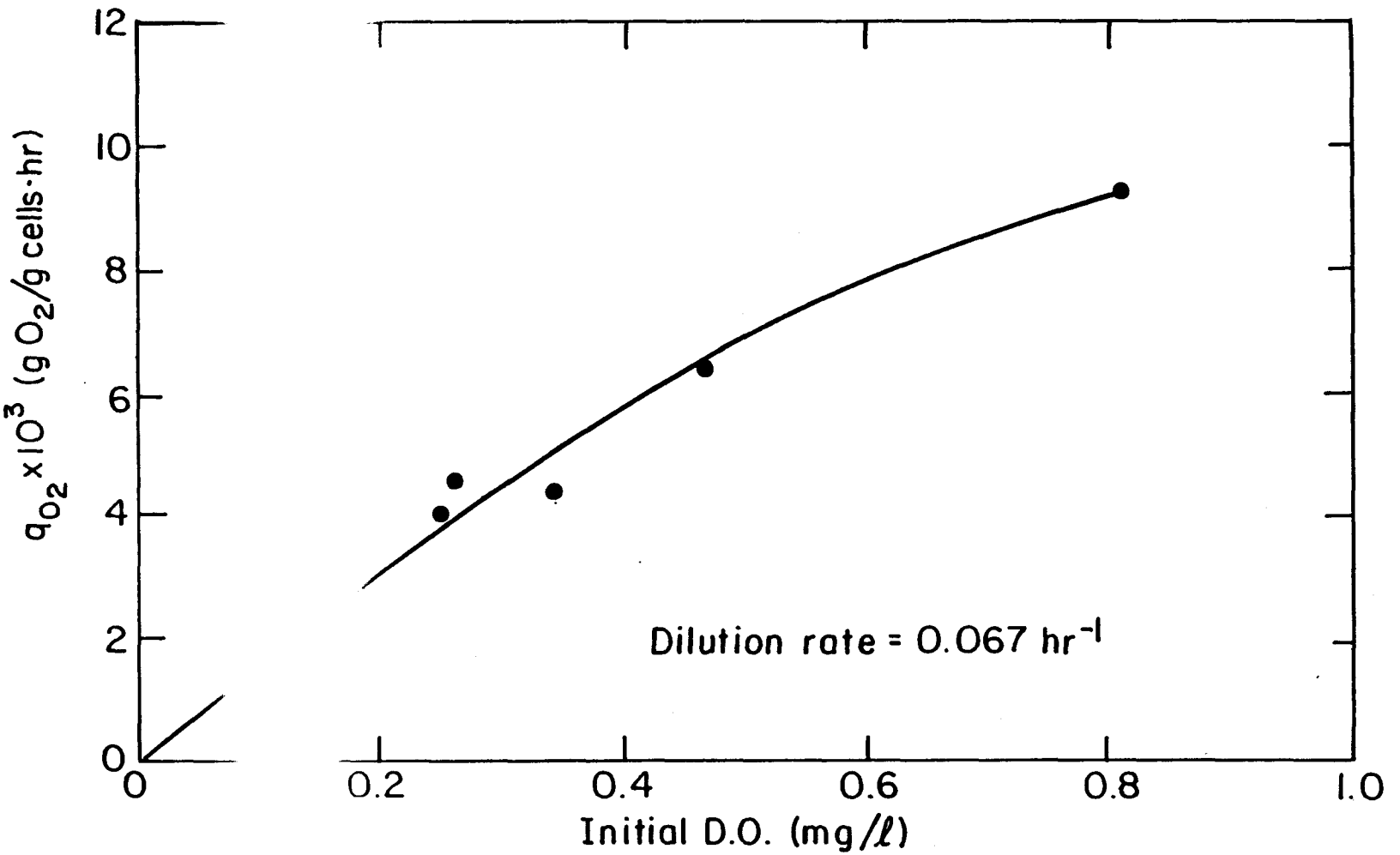

XBL822-5279

Figure 1 Specific oxygen consumption versus initial dissolved oxygen at a dilution rate of 0.067/hr.

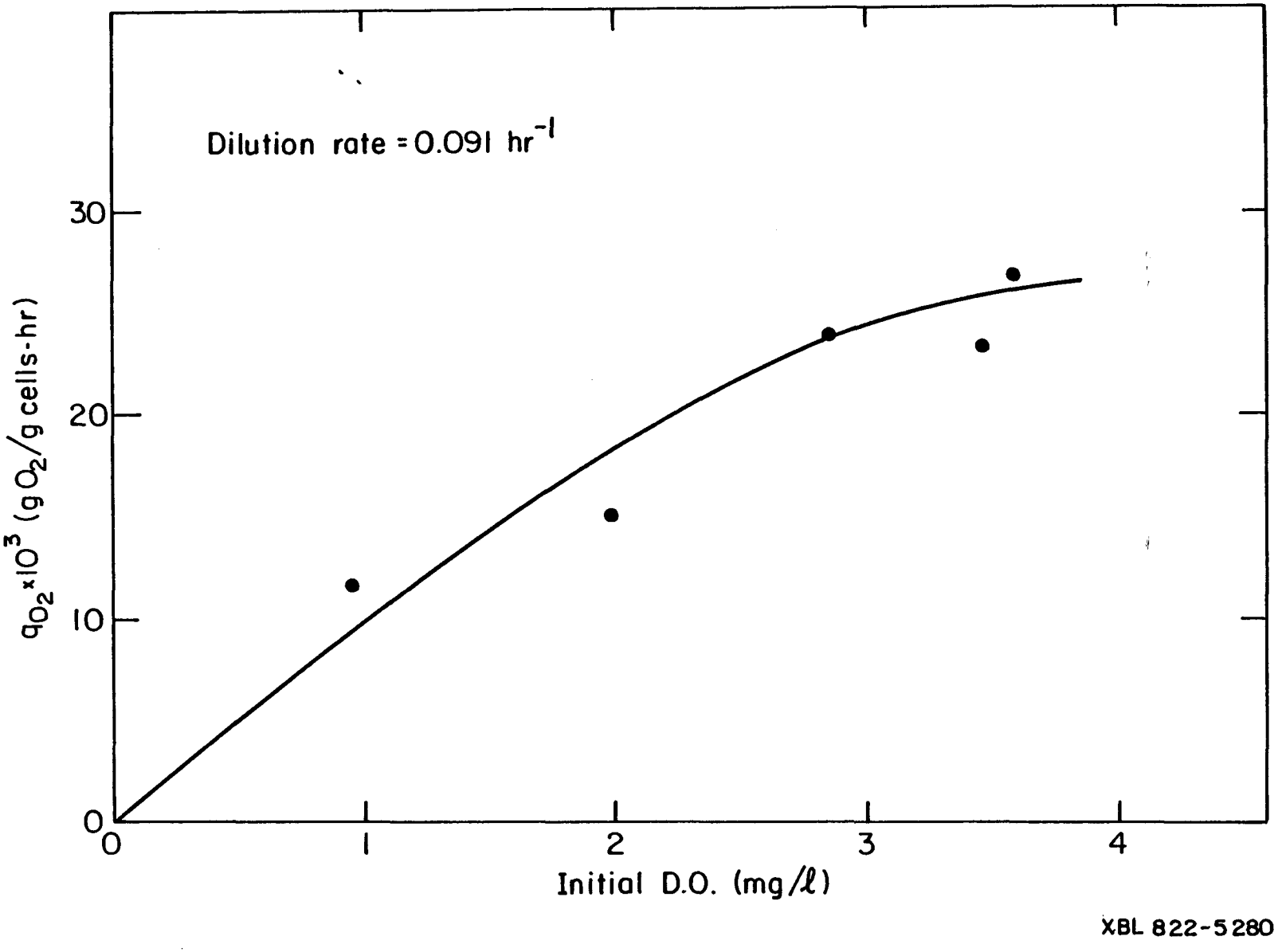

Figure IIB-3. Specific oxygen consumption versus initial dissolved oxygen at a dilution rate of 0.091/hr.

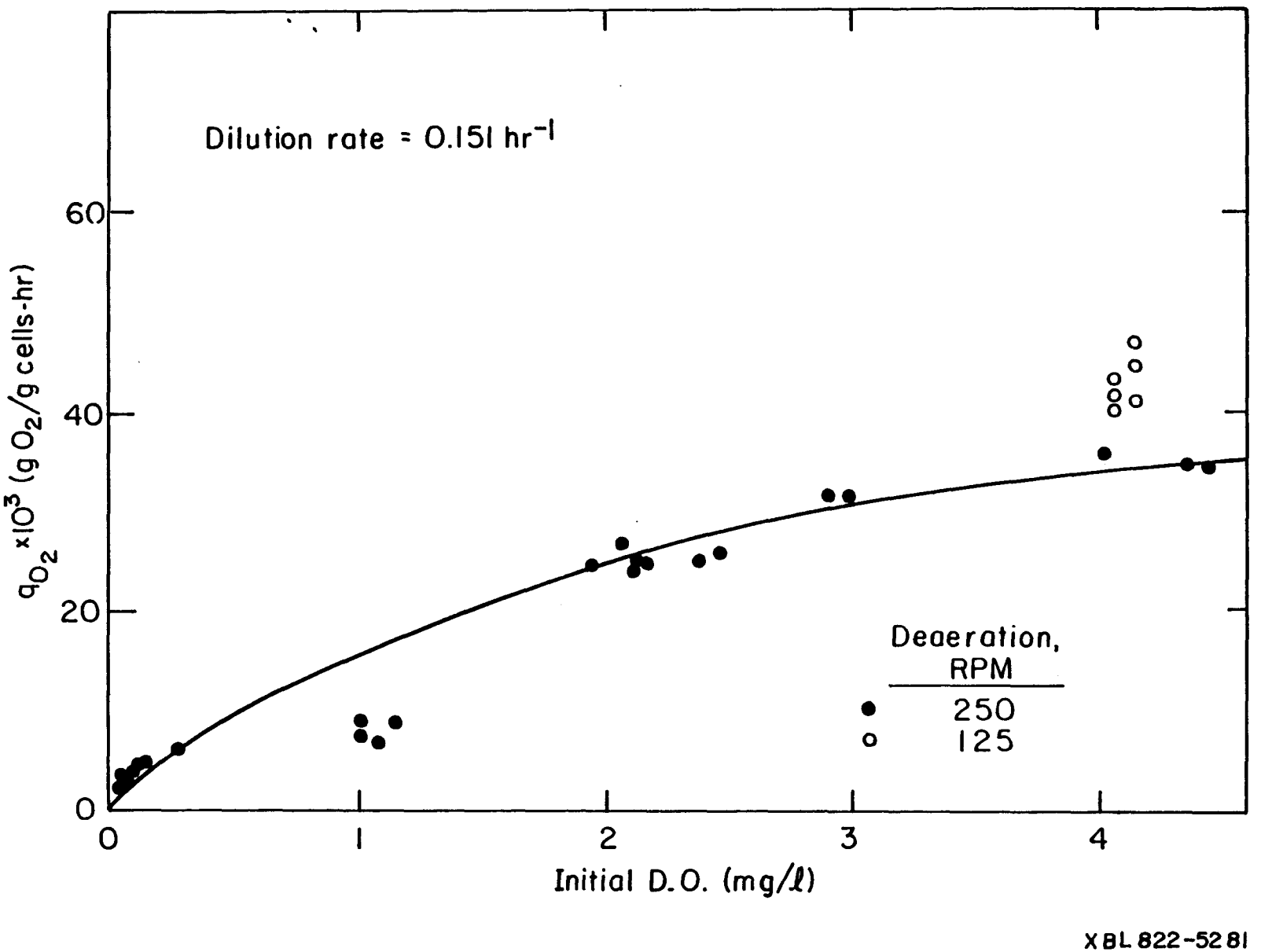

Figure IIB-4. Specific oxygen consumption versus initial dissolved oxygen at a dilution rate of 0.151/hr.

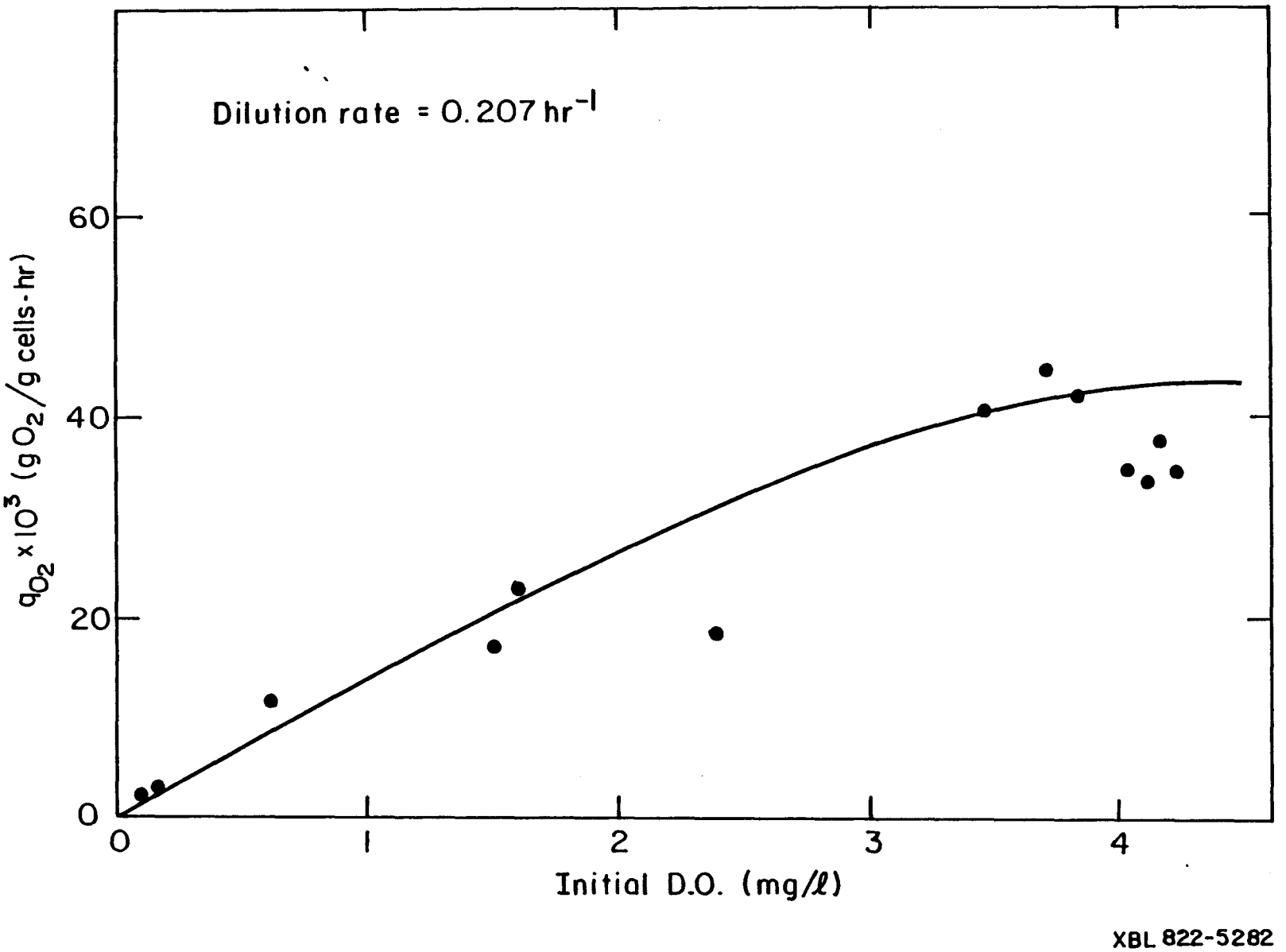

Figure IIB-5. Specific oxygen consumption versus initial dissolved oxygen at a dilution rate of 0.207/hr.

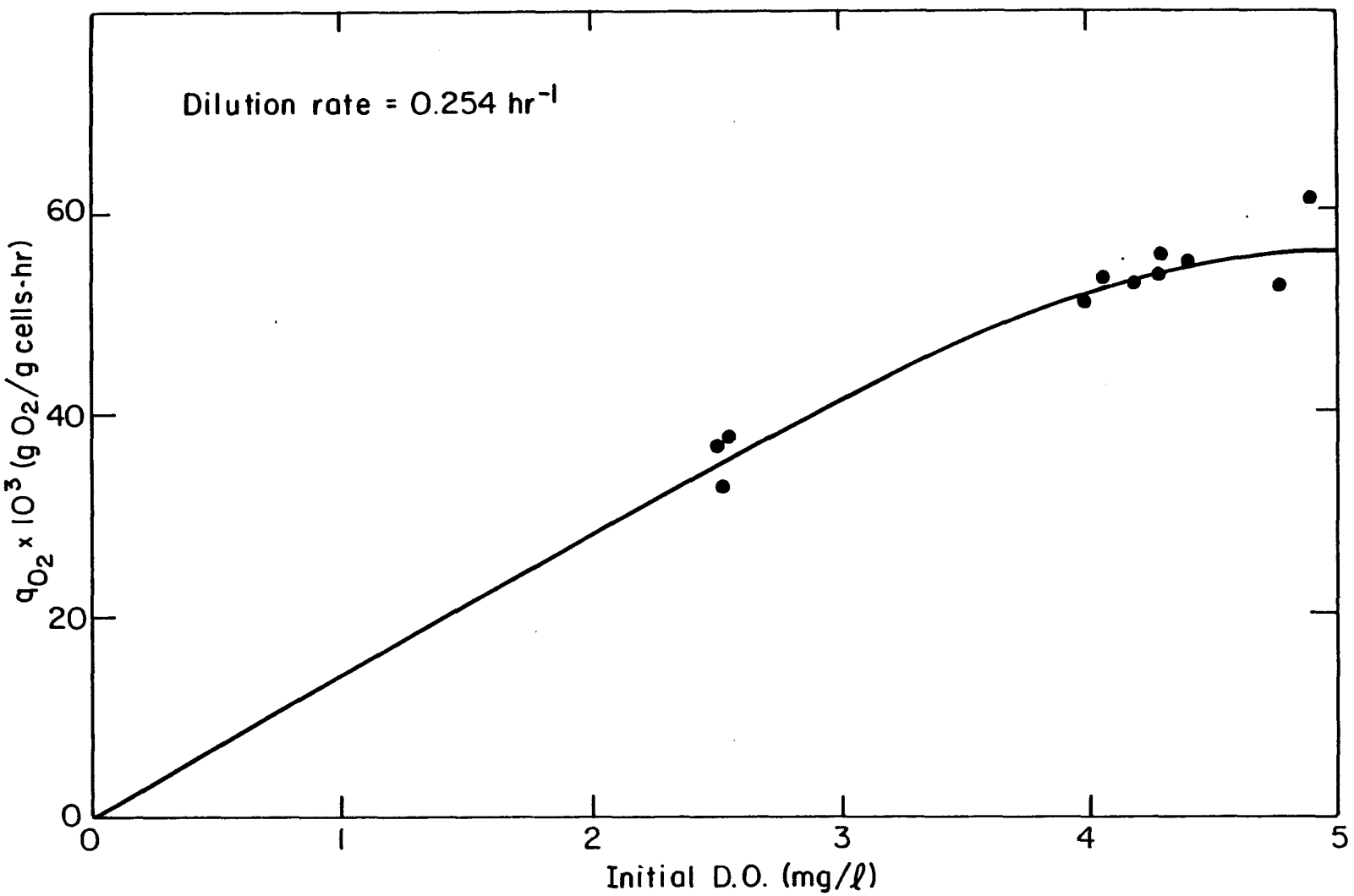

XBL 822-5283

Figure IIB-6. Specific oxygen consumption versus initial dissolved oxygen at a dilution rate of 0.254/hr.

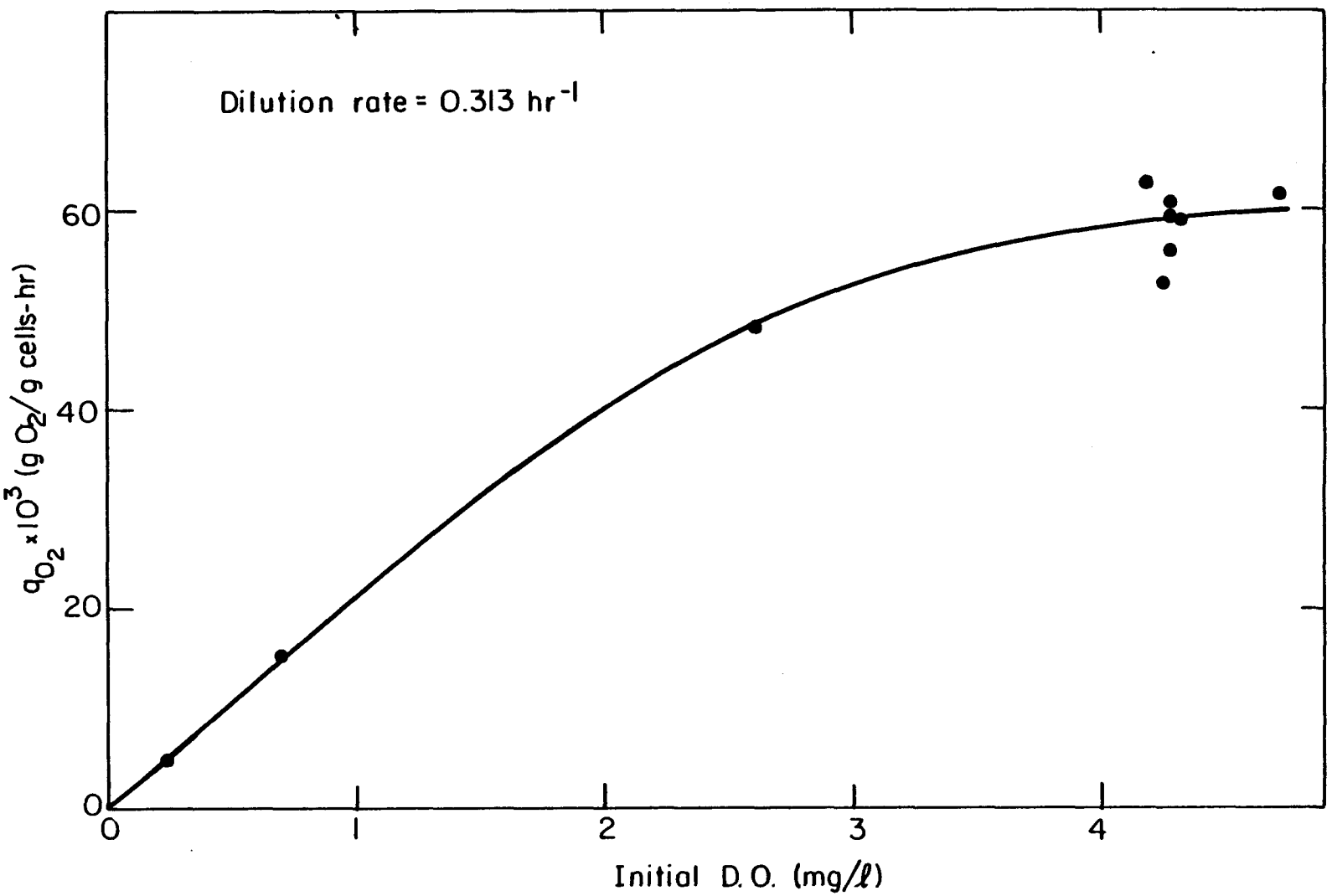

Figure IIB-7. Specific oxygen consumption versus initial dissolved oxygen at a dilution rate of 0.313/hr.

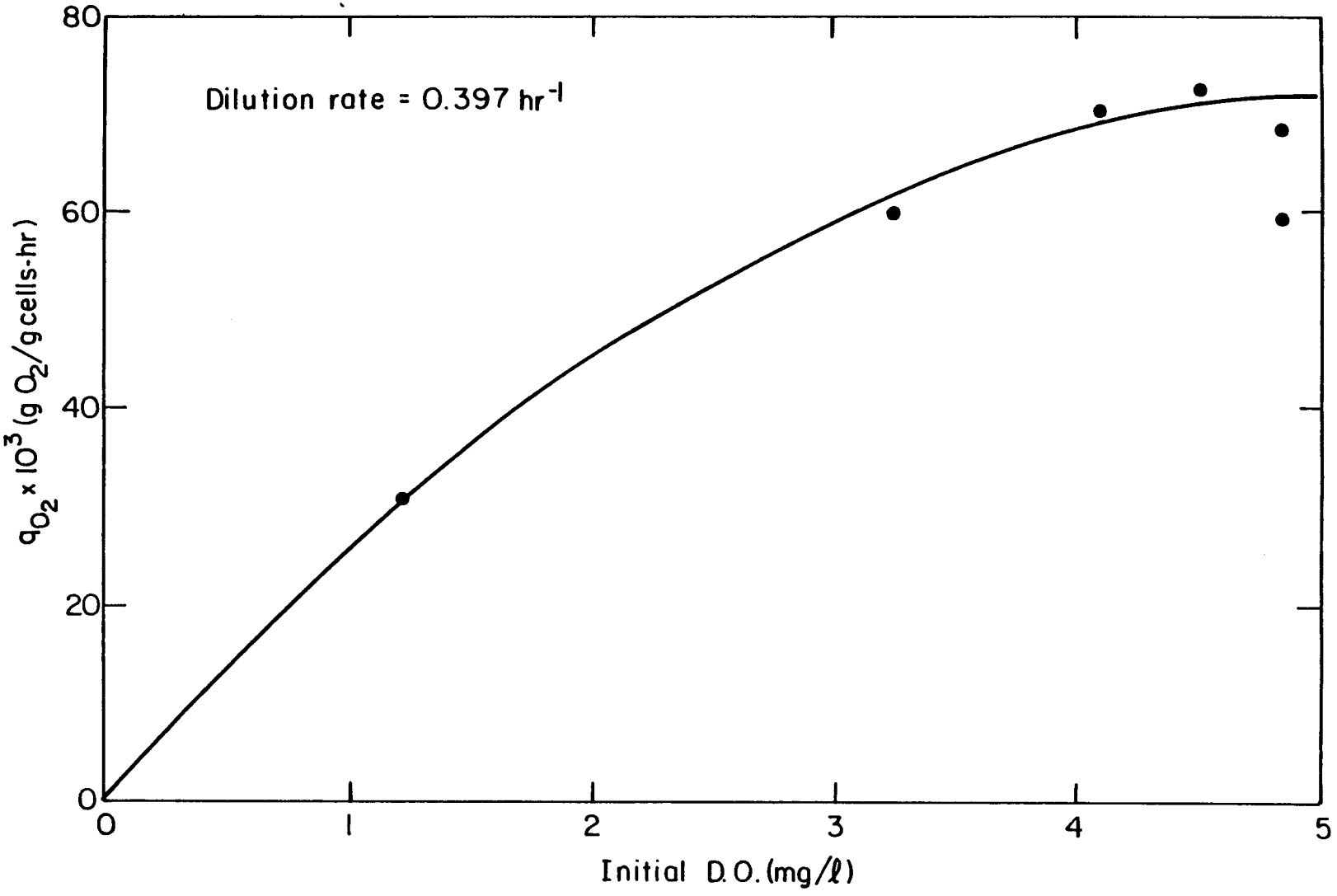

Figure IIB-8. Specific oxygen consumption versus initial dissolved oxygen at a dilution rate of 0.397/hr.

q_{O2} max is the maximum possible specific oxygen consumption rate for a given specific growth rate. However, it is achieved only when the dissolved oxygen concentration is high enough to provide sufficient driving force for transport or for reaction, whichever is rate limiting. The linear relationship in Fig. IIB-9 between q_{O2} max and dilution rate implies that a constant quantity of oxygen is utilized, if available by a given quantity of yeast. This relationship is best quantified with a linear regression, which yields:

$$q_{O2} \text{ max } (hr^{-1}) = 0.0175 + 0.140 \times \text{dilution rate } (hr^{-1}).$$

The slope of this equation implies that 0.140 g O_2/g cells is the maximum oxygen required for growth for dilution rates up to 0.39 hr^{-1}. The intercept gives the maintenance requirement of 0.0175 g O_2/g. cells/hr.

The oxygen requirement for aerobic growth can be determined from the respiratory quotient (RQ) given in Table IIB-1 for each dilution rate. Note that RQ is defined here as the ratio of the mass rate of carbon dioxide production to the mass rate of oxygen utilization. Defining F as the fraction of glucose ($C_6H_{12}O_6$) fermented, RQ can be derived by multiplying Harrison'saerobic growth equation by (1-F) and his fermentation equation by F and then adding these together to yield in terms of glucose, oxygen, and carbon dioxide only:

100g $C_6H_{12}O_6$ + 46.63g (1-F) O_2 +...⟶[67.42g(1-F)+45.32gF] CO2 +..

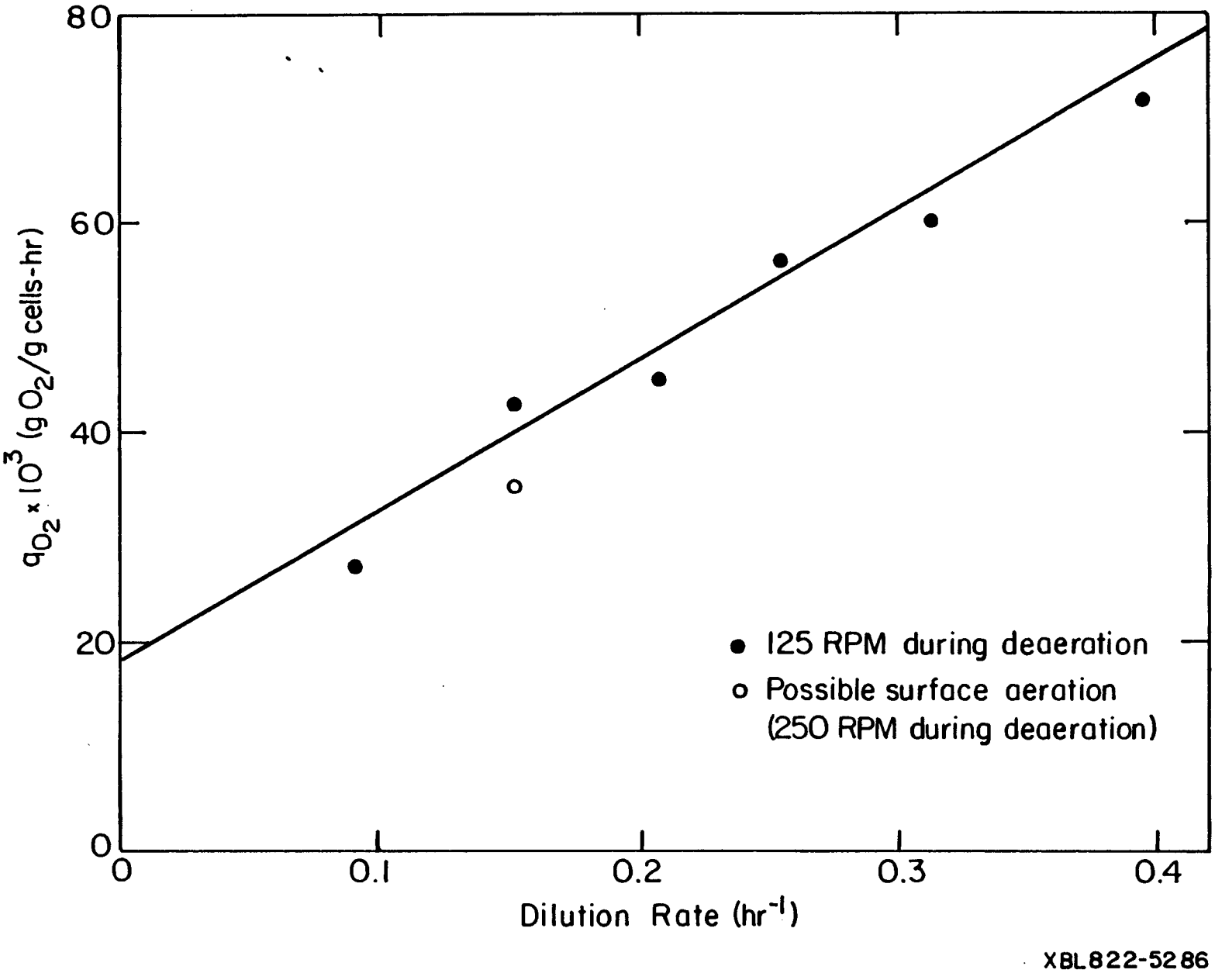

Figure IIB-9. Maximum specific oxygen consumption versus dilution rate.

Table IIB-1

RQ, F, Fermentative Oxygen Usage, and ν

as Functions of Dilution Rate

Dilution Rate (hr^{-1})	RQ (Mass Respiratory Quotient)	F (Fraction Glucose Fermented)	Fermentative Oxygen Usage (mg O_2/g cells)	ν (Specific Ethanol Productivity, g Etoh/g cell/hr)
0.091	15.6	0.936	70.9	0.295
0.151	17.0	0.941	76.3	0.433
0.207	18.2	0.945	80.7	0.633
0.254	16.2	0.938	73.1	0.723
0.313	16.8	0.940	75.3	0.724
0.397	19.7	0.949	85.0	1.095

$$RQ = [67.42(1-F) + (45.32F)/46.63(1-F)]$$

Rearranging,

$$F = (67.42-46.63\ RQ)/22.10-46.53\ RQ)$$

RQ can range from 1.446 to infinity corresponding to F=0 (completely aerobic growth) to F = 1 (completely fermentative growth). The values of F are also given in Table IIB-1 and shows that 93.6% to 94.9% of the glucose was fermented over the range of dilution rates. From Harrison's aerobic growth equation, the aerobic oxygen demand is then

$$(1-F)(46.63/43.23)\ g\ O_2/g\ cells$$

The oxygen usage for fermentation is then the difference between the total usage and the aerobic usage:

$$0.140-1.079\ (1-F)\ gO_2/g\ cells$$

These values are listed in Table IIB-1, ranging from 70.9 to 85.0 mg O_2/g cells.

The relationship of specific ethanol productivity, , to specific oxyen consumption is also given in Table IIB-1. From Figure IIB-10, ν , is a linear function of the specific growth rate with both growth associated and non-growth associated requirements. Therefore, ν , is also a

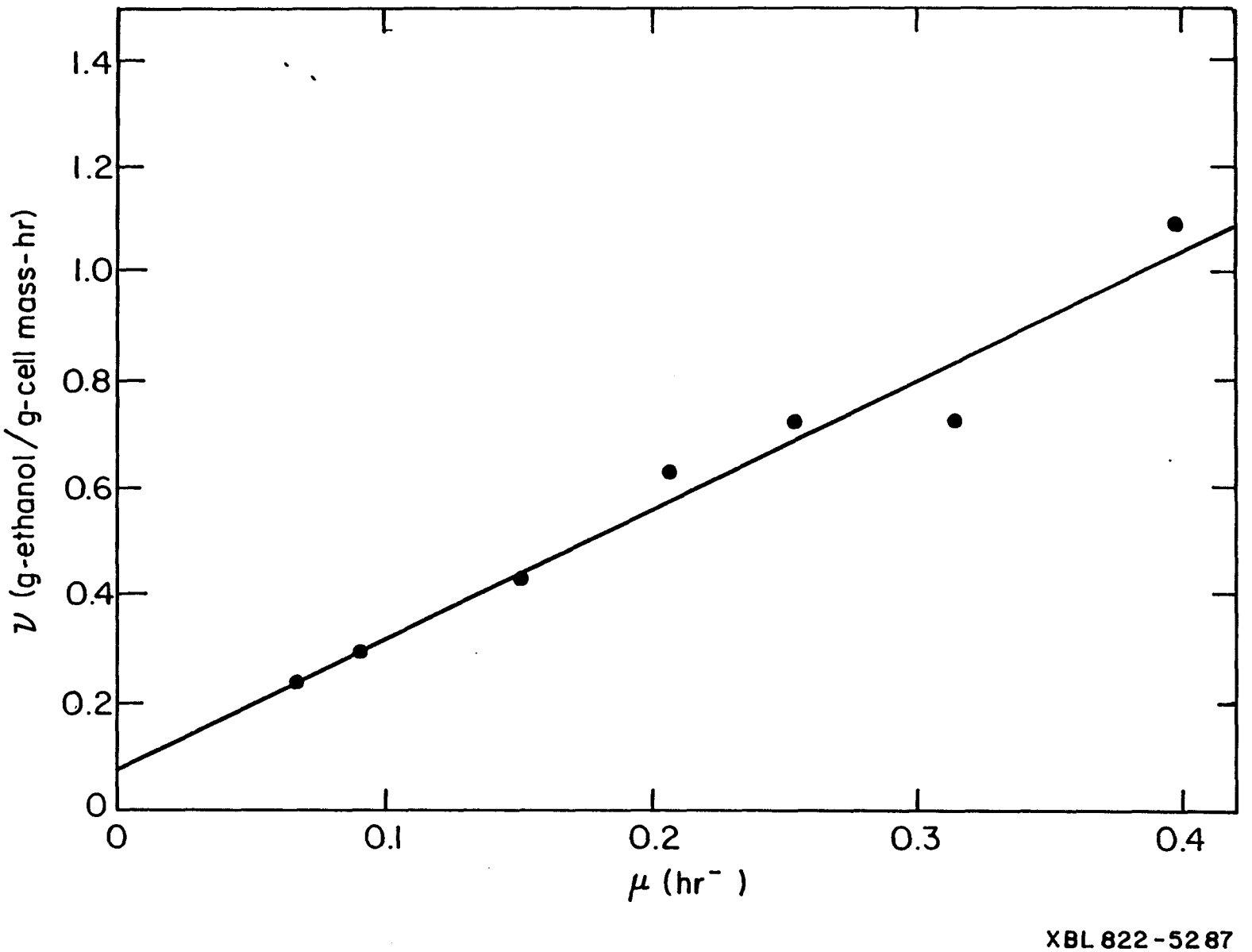

Figure IIB-10. Specific ethanol productivity versus specific growth rate.

linear functon of q_{O2} max.

To understand where oxygen is needed for fermentation and to obtain an order of magnitude estimate of its minimal requirement, the oxygen requirement for synthesizing oleic acid, the predominant unsaturated fatty acid, and ergosterol, the predominant sterol in yeast, can be calculated. Andreasen and Stier (4) showed that 1 g/ml oleic acid was the minimum concentration to produce about 10 million cells/ml under conditions of only oleic acid limiting growth. Andreasen and Stier (8) also showed that between 7 mg/l to 70 mg/l ergosterol, the same order of magnitude cells, 110-125 million cells/ml, were obtained.

In the fermentation of oleic acid molecular oxygen is required by oxidase as shown in the following reaction by Stryer (9):

$$\text{Stearoyl CoA} + \text{NADH} + H^+ + O_2 \xrightarrow{\text{oxidase}} \text{oleoyl CoA} + NAD^+ + 2H_2O$$

Therefore, assuming Andreasen and Stier's oleic acid usage requirement and assuming 10^{-11} gram/cell, 1.1 mg oxygen/gram cells are required for oleic acid synthesis.

In the synthesis of ergosterol (Figure IIB-11) molecular oxygen is first required for the reaction of one molecule of sgualene with one molecule of oxygen to form one molecule of squalene 2,3-epoxide, which this is cyclized to lanosterol (Stryer (10)). Hunter and Rose (11) reported two possible mechanisms for adding the second double bond (at 5-6)

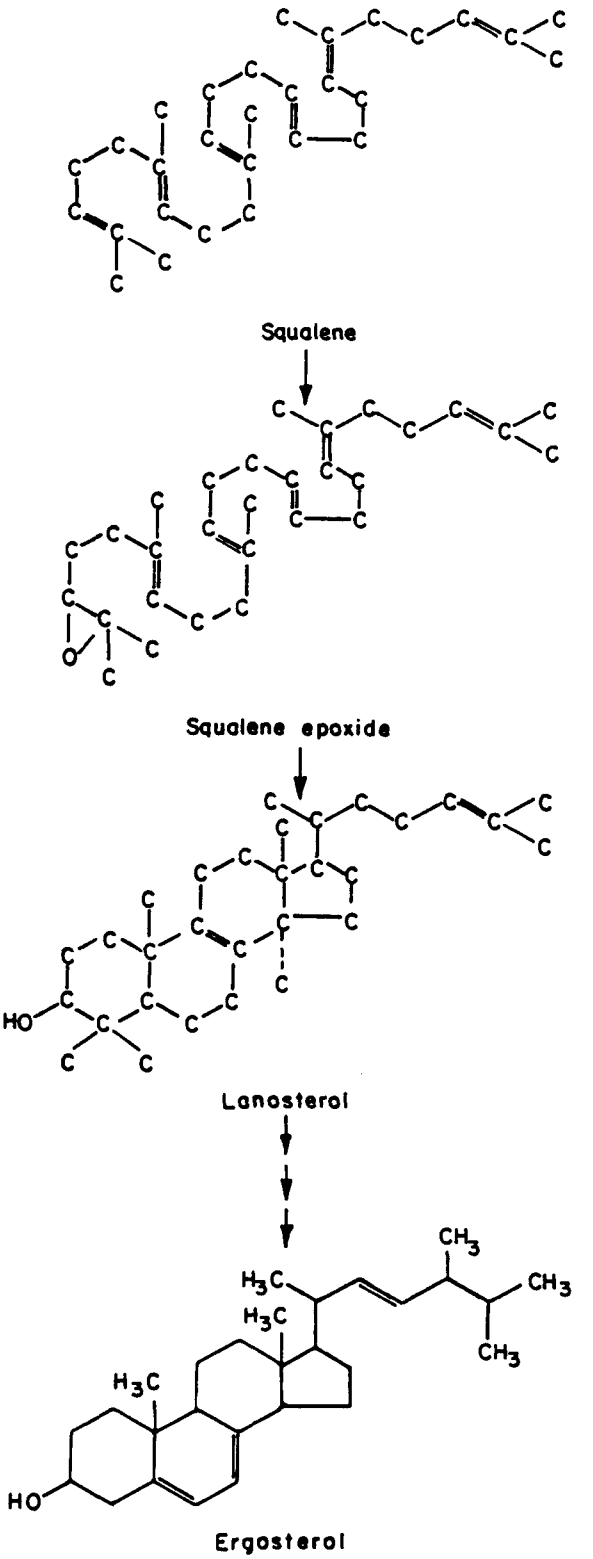

BIOSYNTHESIS OF ERGOSTEROL

XBL822-5288

Figure IIB-11.

into ring B of lanosterol for conversion to ergosterol. One is a hydroxylation-dehydration mechanism, which requires reduced nicotinamide nucleotide and one molecule of oxygen per molecule of ergosterol. The second mechanism also requires oxygen for an overall cis-elimination of two hydrogen atoms. Therefore, at least two molecules of oxygen are required for each molecule of ergosterol. Using Andreasen and Stier's (8) 7 mg/L ergosterol usage requirement for 110 million cells/ml, 1.0 mg oxygen/gram cells are required for ergosterol synthesis.

The combined oxygen requirement for oleic acid and ergosterol is 2.1 mg oxygen/gram cells. The fermentative oxygen usages given in Table IIB-1 are in the 70.9-85.0 mg oxygen/gram cells range. There are many possible explanations for this discrepancy. One important factor is the variability of cell lipid composition with respect to nutrition aeration and other growth conditions. The above calculations assume 0.6% ergosterol in yeasts. Shaw and Jeffries (12) reported total sterol in yeast to be 0.1-1.0%. Dulaney, Stapley, and Simpf (13) reported a strain of S. cerevisiae attaining 7-10% of cell dry weight as ergosterol under certain conditions. High carbohydrate concentrations, sub-optimum nitrogen concentrations and phosphate deficiencies enhance lipid formationn (Hunter and Rose (14)). The ergosterol usage reported by Andreasen and Stier (8) were for yeast grown in a basal medium of Difco yeast nitrogen base, sodium succinate buffer, and glucose. This synthetic medium contains sufficient nitrogen and phosphate, but no carbohydrates. In contrast, the medium used for the experimentally measured

oxygen consumption reported in this paper contains carbohydrates and other carbon sources in the yeast extract, about the same amount of nitrogen and no phosphates. Therefore, it should produce more lipid and require more oxygen.

A second major difference comes from comparing the maximum possible usage of oxygen derived from q_{02} max values measured at oxygen saturation conditions against possible less than maximal ergosterol and oleic acid usages. Andreasen and Stier (8) obtained only about one-third of the cell growth with ergosterol and Tween 80 as with the unsaponifiable fraction of wheat germ oil added to a crude medium containing yeast extract. There may have been other growth limiting factors.

A third source of discrepancy is the unaccounted for use of oxygen either in ergosterol and unsaturated fatty acid synthesis or other biosynthetic processes which utilize oxygen if available but does not require it as an essential element.

4. Future Research on Other Models of Yeast Growth and Ethanol Production.

Future work will be directed at explaining the unaccounted for use of oxygen during fermentation and investigating the transport mechanism for oxygen into the cells. Preliminary calculations indicate passive diffusion is sufficient to satisfy oxygen requirements for the fermentative conditions used.

In addition to studying the effects of oxygen uptake, the effects of varying dissolved oxygen tension will be studied to determine if there is an optimum value for maximum

ethanol productivity and yield. The dissolved oxygen range to be studied will be from below the detectable limits of current probes to the toxic levels much above atmospheric conditions. As a method for determining dissolved oxygen from measurements of the gas phase oxygen concentration, fermentor mass transfer characteristics for oxygen will be studied. In particular the effect of CO_2 on the degree of mixing in the gas phase will be examined.

Other environment effects to be further studied are glucose inhibition, ethanol inhibition, and carbon dioxide inhibition. Glucose inhibition will be studied in batch culture with initial concentrations from 100 g/L to 400 g/L. The ethanol inhibition study will first check de Bazua's model (15), then determine the inhibition effects with the biotin, pantothenic acid, pyridoxine, and thiamine supplemented minimal medium describe in Basic Studies on Yeast Nutrition above. The effect of carbon dioxide will be examined from about 10% to about 90% by volume in the fermentor headspace.

C. By-Product Inhibition in Cell Recycle and Vacuum Fermentation

Inhibition by secondary fermentation products may be limit the ultimate productivity of new glucose to ethanol fermentation processes. New processes are under development whereby ethanol is selectively removed from the fermenting broth to eliminate ethanol inhibition effects. These processes can concentrate minor secondary products to the point where they become toxic to the yeast. Vacuum fermentation selectively concentrates nonvolatile products in the fermentation broth. Membrane fermentation systems may concentrate large molecules which are sterically blocked from membrane transport. Extractive fermentation systems, employing nonpolar solvents, may concenrate small organic acids. By-product production rates and inhibition levels in continuous fermentation with Saccharomyces cerevisiae have been determined for acetaldehyde; glycerol; formic, lactic and acetic acids; 1-propanol; 2-methyl-1-butanediol; and 2,3-butanediol; to assess the potential effects of these by-products on new fermentation processes. Mechanisms are proposed for the various inhibition effects observed.

Enclosed, with this report is a copy of LBl-13343 which was presented at the American Chemical Society Meeting on August, 27, 1981 at New York City.

D. Hollow Fiber Reactor

1. Introduction

High density fermentations can, in principle, lead to higher productivities per unit fermentor volume, the extreme case being a condition where the entire fermentor volume is occupied by microorganisms. The specific productivity of the cells must be maintained at a maximum in order to reap any benefits from this situation. Unfortunately, in conventional fermentors, the kinetics of high density fermentations are usually mass transfer controlled because the high viscosities encountered lead to inefficient mixing. Removal of inhibiting metabolic products is also subject to the same poor mass transfer conditions. A hollow fiber reactor can distribute the nutrients in close proximity to the cells and simultaneously remove waste products by means of semipermeable hollow fiber membranes as shown in Figure IID-1. The microbes are too large to pass through the membrane and are immobilized on the outside of the fibers. The unit functions analogously to the capillaries in the tissue of higher multicellular organisms. By distributing the nutrient broth to the cells, the mass transfer limitations of high viscosity systems are circumvented. Additional advantages of this fermentor over conventional equipment are that it provides an *in situ* separation of cells from the product stream, it imposes no shear on the cells, and it is completely resistant to washout. Furthermore, if a 'resting state' can be obtained where the cells are actively producing product yet not growing, then greater product yields may be realized.

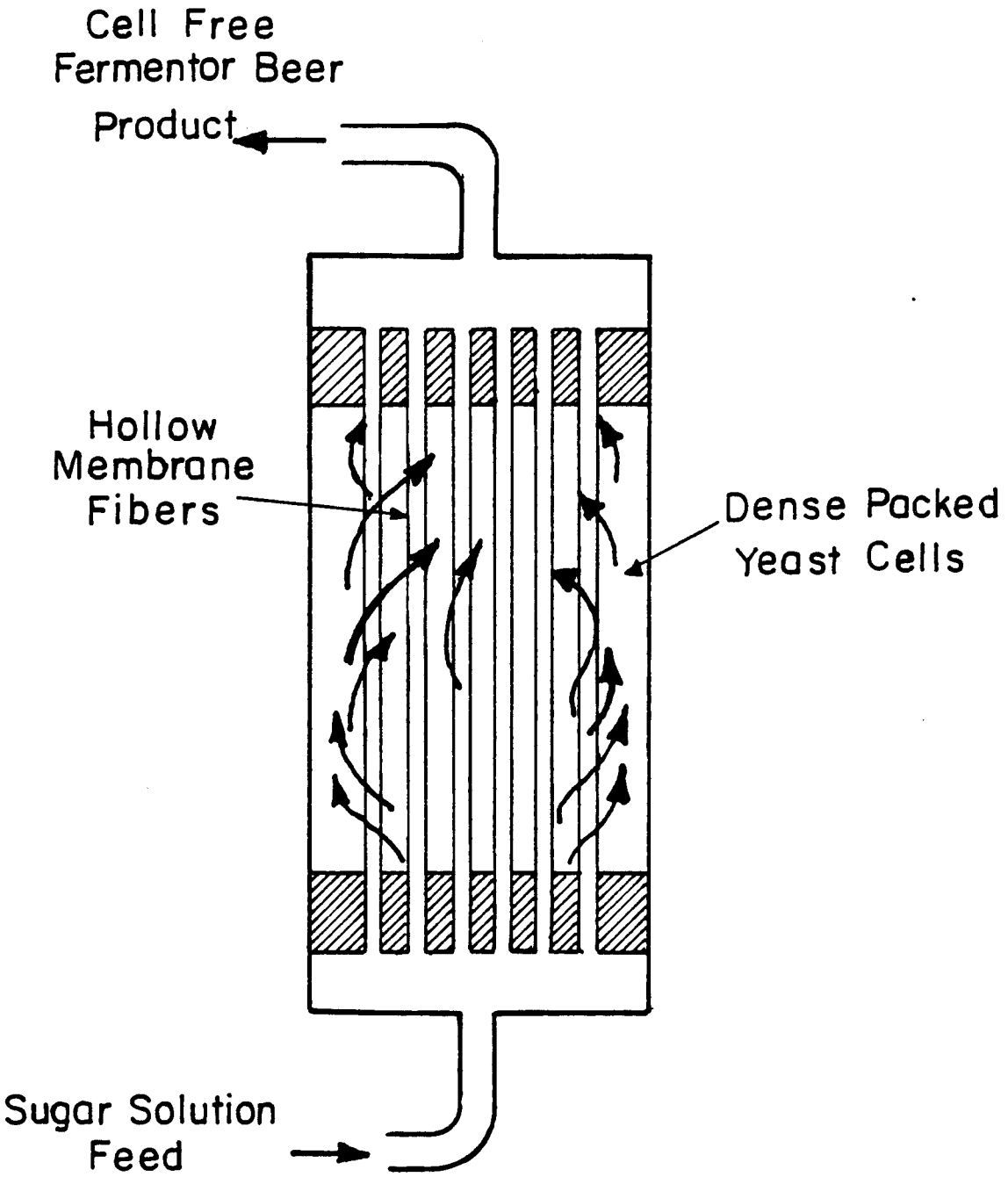

Hollow Fiber Fermentor

XBL 803-4899

Figure IID-1.

2. Current Research

It has been observed that 'channeling' of the flow through a fraction of the available fibers can occur which would have serious consequences on the distribution of nutrients to the cells. To investigate channeling flow studies using dye tracers were performed with Amicon, 100,000 MW cutoff, polysulfone fibers. These studies were hampered by cartridge leaks but indicated that clogging of the fibers by particulates is important at all flow rates. Gas bubbles in th fibers may block the flow at low flow rates. Pre-filtering of the medium with a 10-15 μM pore glass frit will be used in all subsequent runs.

A yeast fermentation was performed in a unit with two sets of fibers. One set was used to deliver the nutrients to the culture and the other set was used to remove the fermentation products. The fermentation never proceeded very far because of extreme fouling of the product tubes. This fouling was assumed to be caused by a layer of compacted yeast cells, and macromolecules from the yeast extract. Compaction of the membranes (Amicon 100,000 MW polysulfone) was also responsible for part of the fouling. After being exposed to a pressure differential of 6.0 psi or greater the shell to lumen flux rate decreased by about 50% as fouling developed. Lumen to shell flux rates were not affected.

Venting the fermentation gases, i.e., CO_2) from the shell side poses numerous problems. The thicker the cell suspension becomes, the harder it is to remove the gas. In the above experiment the rate of gas evolution was sufficient enough

to entrain liquid from the shell side. The volume occupied by the gas lowers the volumetric productivity of the device. Attempts to circumvent the gas evolution problem by cyclic vacuum, increasing the shell side pressure and vibration were unsuccessful. A literature search for non-gas evolving biosystems and/or slowly growing systems was made. The results of this search showed that there are three kinds of fermentations suitable for this device. In the first type of fermentation the cells are growing to produce some particular enzymes and then lysed. The system is then used as a whole cell immobilized enzyme reactor. In the second kind of fermentation no gas is evolved. In the third type of fermentation, gas may be evolved but at a rate slow enough that it is absorbed by the liquid. Some specific systems that appear to be applicable to this fermentor are lactic acid fermentations, and plant and animal tissue culture.

For further studies of the fermentor, Lactobacillus delbreuckii NRRL B-445 was chosen. Batch runs indicated the organism obtained behaves in agreement with the data already in the literature (1,2). The organism does absorb oxygen from the medium, although its growth yield and lactic acid yield remain the same. Lactic acid is measured by an enzymatic method. The organisms appear to produce mostly L(+) lactic acid and about 2% D(-) lactic acid.

A hollow fiber fermentation was performed. Sixty 150 μM o.d. Celanese Celard fibers were used in an Amicon Vitafiber unit. Many particles were caught by the 10-15 μM prefilter even

though the medium was filter sterilized. The production rate of the unit achieved was only 10% of maximum. A pH drop of one unit was observed over the cartridge. The growth optimum of the organism is only from pH 5.6 to 6.0, so this could be a major reason for the low production rate. The cells grew very densely around the fibers. The fibers did not plug or collapse throughout 4 days of operation.

Work with the Celanese fibers was delayed because of difficulties in potting these fibers. They can now be successfully handled. The fibers performed well in the first fermentation. Despite their small diameter they did not plug. Cells did not penetrate the fibers and no collapse of the fibers was noticed.

3. Future Research

Several more hollow fiber fermentations will be performed. Stronger buffering and/or higher flow rates through the fibers will reduce the pH drop over the cartridge. The experiments will also examine the major design variables of such fermentors including fiber types, fiber size, spacing between fibers, cartridge length, and fiber lumen flow rates. Further studies of the organisms behavior in a 'resting state' is pertinent to the success of this fermentor. Such resting states may be achieved by limiting the nitrogen source in the feed and/or adding toxins to the medium.

To characterize the flow and mass transfer in the unit, some further flow studies will be done and the tortuosity of the Celanese fiber walls will be measured. These tortuosity

measurements are presently under way, and the diffusion of several types of molecules through these hydrophobic microporous fibers will be examined.

References

1. Hanson, T.P. and G.T. Tsao, Biotechnol. Bioeng. Vol. 14, 233-252 (1972).

2. Luedeking, Robert and Edgar L. Pivet, J. of Biochemical and Microbiology Tech. and Eng. Vol. 1 393-412 (1959).

A. Ethanol/Water, Physical/Chemical Properties-- Compilation and Critical Evaluation

1. Introduction

Accurate property data are essential for the design and evaluation of new ethanol/water separation processes. This section provides a compilation of important physical, chemical, and thermodynamic properties of ethanol, water, and their mixtures. Property data are also included for major fermentation by-products which can effect the ethanol/water separation design. Data for selected separating agents is also included.

Preparation of data for this compilation involved four steps. 1) Where available, data were collected from the chemical literature; 2) All data were critically reviewed (as in the case for ethanol/water-vapor/liquid equilibrium data, where thermodynamic consistency testing was used to eliminate faulty data sets); 3) Data were correlated and computer routines developed to allow ready application in process screening and design; and 4) Where important data were not available in the literature (as in the effect of biological components and whole yeast cells on ethanol/water equilibrium properties), new experiments were conducted to collect the required data.

For vapor/liquid equilibria the model to be used will be the general thermodynamic relationship:

$$Y_i \, \phi_i \, P^{total} = X_i \, \gamma_i \, f_i^{0,liq} \exp[P^{total} V^{liq}/(RT)] \qquad (1\text{-}1)$$

where:

Y_i = mole fraction component i in vapor

X_i = mole fraction component i in liquid

p^{total} = system total pressure

γ_i = liquid phase activity coefficient for component i

$f_i^{0,liq}$ = zero pressure reference fugacity for component i in the liquid

v_i^{liq} = partial molar volume of component i in the liquid

Many of the correlations given in the following sections are chosen to lead to this overall model.

To be of the greatest use in process screening and design, property data must be in computer usable form. The integrated computational package of Prausnitz, et al. (1) is a versatile system for thermodynamic property evaluation and is used widely in industry. Whenever possible, correlations and new computer subroutines have been chosen to be compatible with this package. Where correlations used in this package were found inferior to others available (such as for liquid densities) both correlations are included.

2. Basic Property Data

This section presents basic physical property constants for ethanol and water. Values of these basic properties are well agreed upon. Several of these basic property values will be used in the development of correlations for the further properties discussed in subsequent sections.

a. Ethanol/Water Basic Property Data

Ethanol basic property data are summarized in Table IIIA-1. Water basic proprty data are summarized in Table IIIA-2.

3. Nonideal Vapor Phase-The Fugacity Coefficient

a. Fundamental Equation

The fundamental thermodynamic equation of vapor liquid equilibrium is:

$$f_i^{vap} = f_i^{liq} \qquad (3\text{-}1)$$

where f_i = fugacity of component i in the specified phase

For an ideal system, Raoult's law expresses the vapor/liquid equilibrium relationship as:

$$Y_i P_{total} = X_i P_i^{pure} \qquad (3\text{-}2)$$

where Y_i = mole fraction of component i in the vapor phase

X_i = mole fraction of component i in the liquid phase.

P_{total} = system total pressure

P_i^{pure} = Vapor pressure of pure component i at the system temperature.

For the vapor phase, this is equivalent to assuming the ideal gas law.

Raoult's law fails for all but the simplest systems. At low to moderate pressures (less than 5 bar) the activity coefficient is generally added to account for liquid phase

TABLE IIIA-1

Ethanol Basic Property Data

Property	Value	References
General Properties:		
Formula	C_2H_5OH	
Molecular Weight	46.069	1,2,3,4,5
Normal Boiling Point	351.47°K	1,2,3,4,5
Melting Point	159.05°K	1,2,3,4,5
Density_4^{20}	0.7893	2,3,4
Flash Point	282-284°K	2,3,4
Surface Tension (298°K)	23.1 dyn/cm	2,4
Association Parameter	1.40	1
Critical Properties:		
Critical Temperature	516.26°K	1,4,5
Critical Pressure	63.835 bar	1,4,5
Critical Volume	167. l/kgmole	1,4,5
Critical Compressibility	0.248	1,4,5
Molecular Properties:		
Dipole Moment	1.69 debye	1,5
Radius of Gyration	2.2495Å	1,5
Pitzer Acentric Factor	0.635	5
Thermodynamic Properties:		
Heat of Combustion (298°K)	326.8 Kcal/gmole	2,4
Heat of Fusion	1.152 Kcal/gmole	2,4
Heat of Formation (298°K)	-56.12 Kcal/gmole	2,5
Gibbs Energy of Formation (298°K)	-40.22 Kcal/gmole	2

Table IIIA-2

Water Basic Property Data

Property	Value	Reference
General Properties:		
Formula	H_2O	
Molecular Weight	18.016	1,2,5
Normal Boiling Point	373.15°K	1,3,5
Melting Point	273.15°K	1,5
Density $\frac{20}{4}$	1.000	2,3
Surface Tension (298°K)	73. dyn/cm	2
Association Parameter	1.70	1
Critical Properties:		
Critical Temperature	647.37°K	1,5
Critical Pressure	221.20 bar	1,5
Critical Volume	56.0 l/kgmole	1,5
Critical Compressibility	0.229	1,5
Molecular Properties:		
Dipole Moment	1.83 Debye	1,5
Radius of Gyration	0.6150Å	1,5
Pitzer Acentric Factor	0.344	5
Thermodynamic Properties:		
Heat of Fusion	1.435 Kcal/gmole	2,3
Heat of Formation (298°K)	-57.80 Kcal/gmole	2,5
Gibbs Energy of Formation (298°K)	-57.64 Kcal/gmole	2,5

nonideality, but no correction is made for the vapor phase. For the system ethanol/water, however, polar interactions increase the vapor phase nonidealities and even at 1 bar pressure, a fugacity correction is necessary.

$$\Phi_i \, Y_i \, P_{total} = \gamma_i \, X_i \, f_i^{ref,liq} \qquad (3\text{-}3)$$

where Φ_i = component i, gas phase fugacity coefficient

γ_i = component i, liquid phase activity coefficient

$f_i^{ref,liq}$ = reference fugacity for component i in the liquid at standard state conditions for γ_i

In this section, the Hayden-O'Connell virial equation correlation for fugacity coefficients is outlined and evaluated for the system ethanol/water. A later section considers the liquid phase nonidealities.

b. <u>The fugacity coefficient from an equation of</u> State.

The fugacity coefficient is a function of temperature, composition, and pressure. It relates nonidealities in the vapor phase pressure/volume/temperature relationship and hence, a model for the fugacity coefficient can be developed from any gas phase equation of state which adequately models the vapor P/V/T behavior. In this way, the well developed vapor equation of state correlations may be applied rather than developing an entirely new fugacity correlation.

The relationship between fugacity coefficient and vapor phase P/V/T relations can be developed directly from the definitions of fugacity coefficient and fugacity:

$$\Phi_i = f_i/(Y_i\ P_{total}) \tag{3-4}$$

$$[(\partial \ln f_i/(\partial P)]_T = V_i/RT \tag{3-5}$$

and with suitable thermodynamic manipulations (7), we find

$$RT\ \ln(f_i/(PY_i)) = RT\ \ln\ \phi_i =$$

$$-\int_{\infty}^{V}[(\partial P/\partial n_i)_{T,V,n_j} - (RT/V)]dV - RT\ \ln\ Z \tag{3-6}$$

Any suitable equation of state may now be substituted and fugacity coefficient correlations have been developed based on the Redlich-Kwong, Sugie Lu, Lee-Erbar-Edmunster, Benedict-Webb-Rubin, Pitzer and virial equations of state (5). Only for the virial equation are rigorous thermodynamic relations known for relating mixed component vapor properties to the pure component properties, therefore this equation has been chosen as the starting point in most recent correlations for the fugacity coefficient.

The virial equation is given as

$$Z = PV/(RT) = 1 + B'(T/V) + C'(T/V^2) +... \tag{3-7}$$

Expressed in pressure explicit form and truncated after one term, the virial equation reduces to

$$Z = 1 + B[P/(RT)] \tag{3-8}$$

where P = system pressure

T = system temperature

R = ideal gas constant

Z = compressibility

and the second virial coefficient for a mixture is given by the rule:

$$B = \sum_{i=1}^{n} \sum_{j=1}^{n} Y_i \, Y_j \, B_{ij} \, (T) \qquad (3\text{-}9)$$

derived from statistical mechancis arguments.

This truncated virial equation accurately models the P/V/T behavior of ethanol and water systems (and others) up to about one half their critical density (at which point further terms must be retained). This is well beyond the pressure range of likely distillation and extraction processes. Substituting the virial equation into equation 3-6 (with the appropriate differentiations) yields the desired relation:

$$\ln \phi_i = [2\sum_{j=1}^{n}(Y_j)(B_{ij}) - B(P/RT) \qquad (3\text{-}10)$$

Now, all that is required is an expression for the virial coefficients.

c. Virial coefficient correlation: The Hayden-O'Connel Correlation

The second virial coefficient is a correction to the ideal gas law to consider vapor phase pair interactions. As such, the virial coefficient can be directly related to the

interaction energy between molecular pairs as expressed by a pair potential:

$$B = 2\pi N_o \int_o^{\infty} (1-e^{-(\Phi/kT)}) r^2 dr \qquad (3\text{-}11)$$

where: I = the molecular pair potential function

r = molecular separation distance

k = Boltzman constant

N_o = Avogadro's number

For a simple system with only the classical electrostatic forces (no polar or association contributions) the molecular interactions will be made up of bound, metastable bound and free types (Fig. IIIA-1), and corresponding contributions to the virial coefficient can be considered (7). With no association, the metastable and bound contributions have been correlated with the critical properties, dipole moment (μ), and a molecular size parameter (8).

The free (repulsive, molecular volume) contribution to the virial coefficient has also been correlated for nonpolar nonassociating molecules using only critical properties and the Pitzer acentric factor (to correct for molecular nonspherocity) (9,10). None of these correlations are adequate for the evaluation of virial coefficient for the polar ethanol/water system.

The limitations of previous correlations are overcome by the modification of Hayden and O'Connell (11). In the model, pair interactions are represented in two parts, a

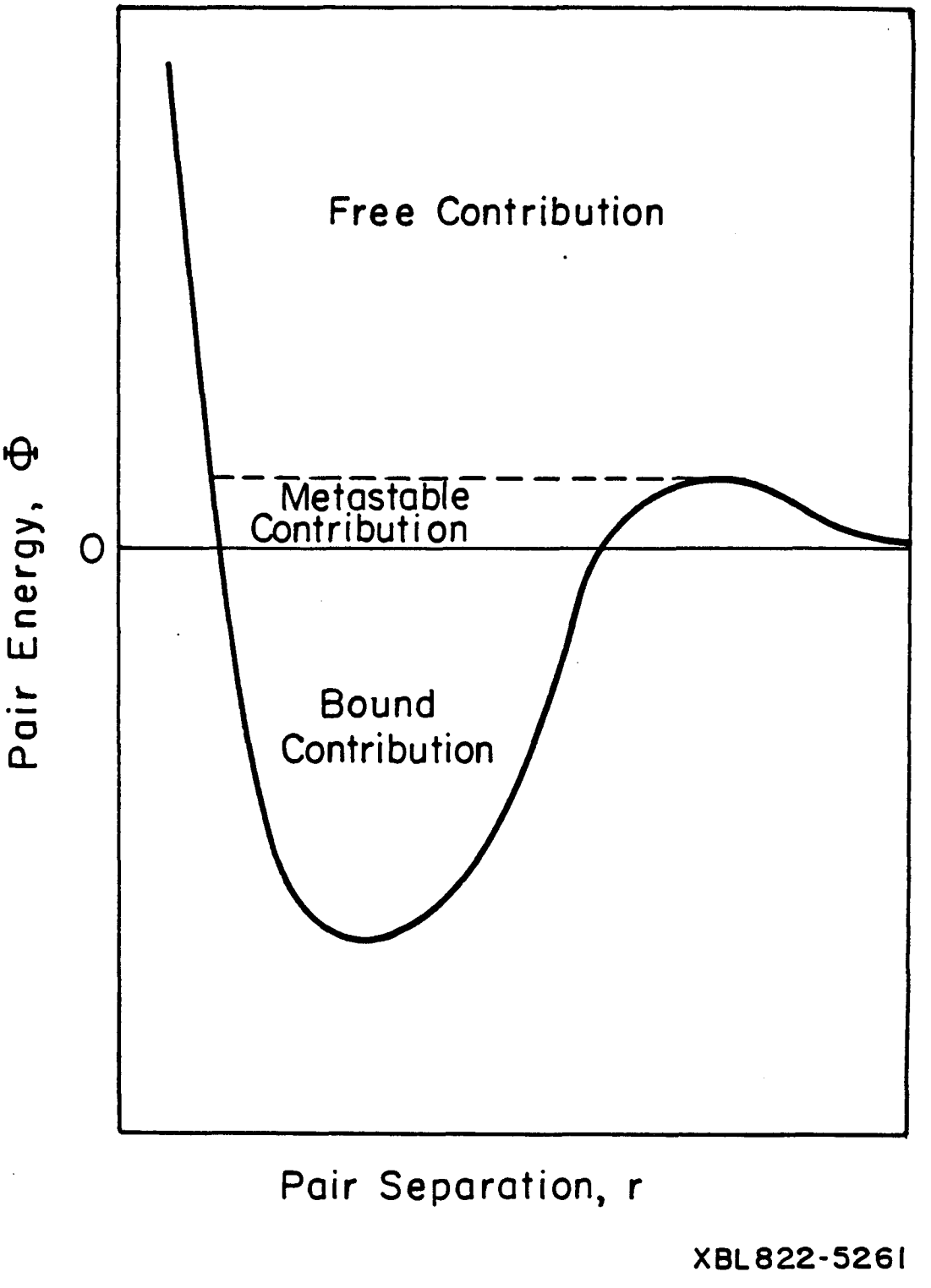

Figure IIIA-1. Simple model of electrostatic pair versus radii of pair separation.

classical electrostatic contribution and the nonclassical contribution arising from polar and association effects. In this way, equations of the forms already developed can be used to correlate most effects. To apply these equations in finding the classical contributions for polar molecules, pseudo-polar reduced properties were developed. For the nonspherocity correction to the free contribution, the Pitzer acentric factor is replaced with the mean radius of gyration (which is not altered by molecular polarity as is the Pitzer factor) and nonpolar changes to the critical temperature and pressure are cancelled by using a molecular dipole moment angle averaging correction to the interaction energy and molcular size correlations.

To complete the correlation for polar and associating components, correlations were developed to account for these additional effects. The polar (attractive) contribution to the free contribution was correlated by empirically fitting data for polar, nonassociating compounds. The association contribution to the bound contribution was then correlated as an equilibrium constant for the association reaction in terms of an association (or solvation for unlike molecules) parameter. For unlike pair interactions, suitable mixing rules were developed.

Only six readily available properties are required to use the Hayden-O'Connell correlation. Extensive tables of these properties are provided in the Appendices of both "The Properties of Gases and Liquids" (5) and "Computer Calculation for Multicomponent Vapor-Liquid and Liquid-Liquid Equilibrium"(1) as well as in other sources. Where measured properties are not

available, predictive methods can be used (5). Required property data for ethanol and water are summarized in Table IIIA-3.

d. Alternative correlations

Alternative relations have been developed to correlate the second virial coefficient for polar systems (12-19). Hayden compares his correlation with those of Nothnagel, Tsonopoulos, Black and Kreglenski. For water and alcohol the Hayden-O'Connell correlation is superior to all but the equation of Tsonopoulos which requires fitting coefficients. The Hayden-O'Connell correlation is very general. It is the correlation employed in the Prausnitz computer equilibrium calculation package. As shown in the following evaluative section, the correlation is excellent.

e. Fugacity Coefficient Computer Implementation

In ETOH (the ethanol/water equilibrium)package, the Hayden-O'Connell correlation is used in determining fugacity coefficients. The virial coefficients are calculated in subroutine TDEP (modeled after subroutine BIS2 in the more general Prausnitz package), and the fugacity coefficients are calculated in PDEP (modeled after subroutine PHIS2 of Prausnitz). For a printout of the virial and fugacity coefficients, MODE-24 should be set equal to 1 when the EtOH package is called.

f. Fugacity Correlation--Critical Evaluation

Second virial coefficient for ethanol and water (but not their mixtures) are available in the literature (20-25). Subroutine TDEP of the ETOH package was used to predict

Table IIIA-3

Property Data for Hayden-O'Connel Correlation

Property	Ethanol	Cross	Water
$T_{critical}$ (°K)	516.26	-	647.37
$P_{critical}$ (bar)	63.835		221.20
Radius of Gyration (Å)	2.250		0.615
Association Parameter	1.40		1.70
Solvation Parameter	-	1.55	-
Dipole Moment (Debye)	1.69	-	1.83

With these units, B_{ij} will be given in $cm^3/g\text{-mol}$.

virial coefficients for the ethanol/water system and the results are plotted against measured values in Figure IIIA-2. The various contributions to the virial coefficients are presented in Table IIIA-4.

Vapor phase P/V/T measurements become very difficult at low pressure (less than 500 mmHg) corresponding to low temperature. For the data of Kretschmer and Wiebe, the authors indicate an expected uncertainty in B of only 5 $cm^3/gmol$ at 373^oK and above, but an uncertainty of greater than 100 $cm^3/gmol$ at 313^oK and below. As can be seen in the figure, the correlation agrees well with the data at moderate temperature, deviating most at low temperatures where the uncertainty in the data is greatest. Fortunately, the fugacity coefficient varies as exponential (P) and larger errors can be tolerated in the virial coefficients at lower pressure, and hence lower temperature.

At 373^oK (the temperature at the base of an atmospheric pressure ethanol/water distillation column) the discrepancies between correlation for $B_{ethanol}$ and B_{water} are -3.10 and -19.50 $cm^3/gmols$. At the respective vapor pressures of the components at these temperatures, these deviations would result in deviations in the fugacity coefficients for the pure components of only 0.0002 in 0.9487 and 0.0006 in 0.9850, respectively. Even at 313.15^oK where the deviation is the greatest between experimental and correlation, a difference of only 0.0029 in 0.9854 results.

Figure IIIA-3 shows the plot of ethanol and water

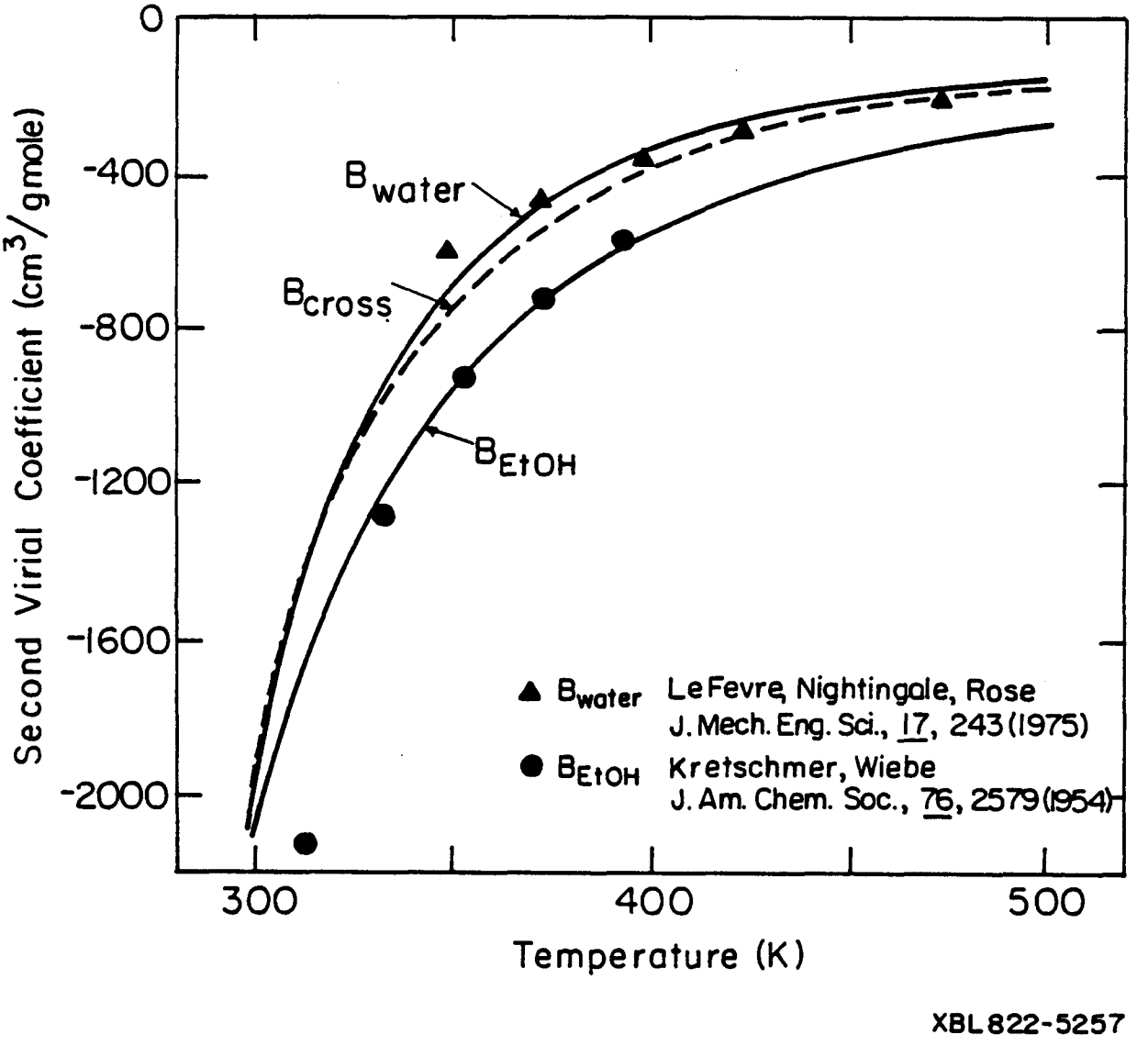

Figure IIIA-2. Calculated second virial coefficients compared to measured values for ethanol/water system.

Table IIIA-4

Second Virial Coefficient Contributions

Contributions	Ethanol			Cross			Water		
	303.15 °K	333.15 °K	363.15°K	303.15°K	333.15°K	363.15°K	303.15°K	333.15°K	363.15°K
B^{free}	-121.8	-88.6	-62.2	-90.5	-57.2	-33.7	- 63.6	-36.6	-18.3
$B^{D,metastable+bound}$	-450.9	-365.2	-306.4	-243.1	-202.0	-173.1	-245.4	-198.9	-166.9
$B^{D,Associative}$	-1400.3	-749.8	-444.9	- 1427.3	-715.1	-401.5	-1486.9	-697.0	-370.2
B	-1973.0	-1203.6	-813.5	-1760.9	-974.3	-608.3	-1795.9	-932.5	-555.8

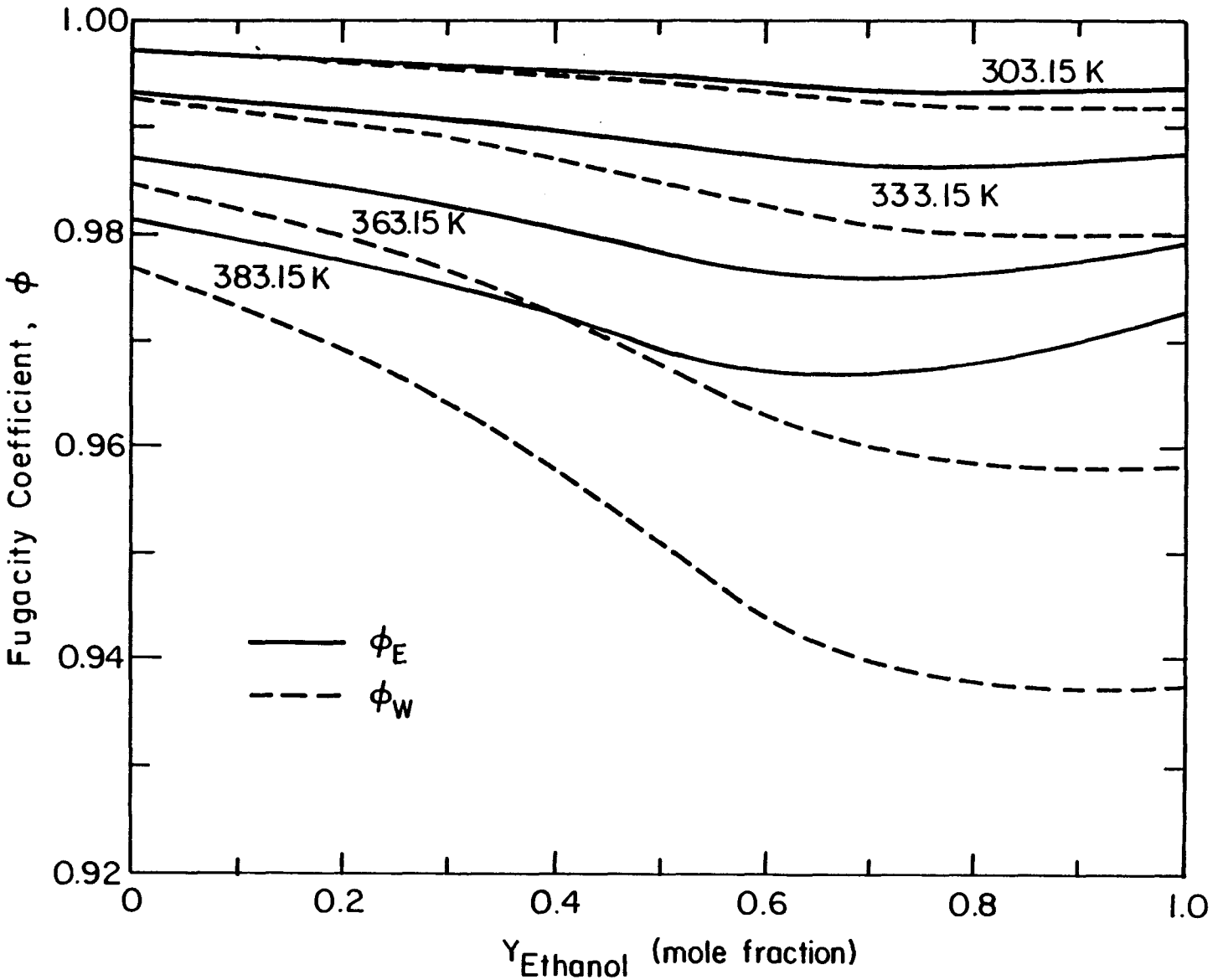

Figure IIIA-3. Fugacity coefficient at saturation pressure for specified composition at temperature.

fugacity coefficients versus mole fraction in ethanol the vapor phase at various pressures and saturation conditions as calculated with subroutine PDEP of ETOH. The temperatures 303 through 383°K cover the likely range for ethanol water separation systems, and it is clear from the substantial deviations from ideality ($\phi \neq 1$) that vapor phase nonidealities cannot be neglected. The vapor fugacity coefficient must be considered in any ethanol/water-vapor/liquid equilibrium evaluation.

4. Liquid Specific Volumes

a. Alternative density Formulations

Ethanol and water densities are necessary for design. The specific volume is also required for the Poynting correction to the vapor/liquid equilibrium relation. Use of a general correlation form which can be applied to other components (preferably without fitting new data) is desirable. Numerous corresponding states formulations have been developed including the Tyn and Calus (26), Chueh and Prausnitz (27) Yamada and Gunn (28), and Rackett (29) equations. Spencer and Danner (30) evaluated the various liquid density equations. For nonpolar liquids these equations could predict liquid densities to within from 5 to 1% accuracy. Substantially larger errors were found for polar liquids.

To predict accurately polar liquid densities, Spencer and Danner (30) proposed a modification to the Rackett (31) corresponding states formulation, employing a single fitting parameter. This modified Rackett parameter is now tabulated for a large number of fluids (1,31), and it can be estimated knowing

only the fluid normal boiling point. The modified Rackett equation is very general (applying to both nonpolar and polar fluids) and is the form used in the Prausnitz equilibrium computation package.

b. The Modified Rackett Equation

The modified Rackett formulation is given by:

$$V_i^L = RT_{ci}Z_{Ri}^T/(P_{ci}) \qquad (4\text{-}1)$$

with

$$= 1 + [1 - (T/T_{ci})]^{0.286} \text{ for } T/(T_{ci}) \ 0.75$$

or

$$= 1.6 + 0.00693/[(T/T_{ci}) - 0.655] \text{ for } T/(T_{ci}) \ 0.75$$

and

$$\rho_i = (MW)_i/(V_i^L) \qquad (4\text{-}2)$$

where

V_i^L = molar volume of pure liquid i

T_{ci} = critical temperature of i

P_{ci} = critical pressure of i

R = ideal gas constant

Z_{Ri} =modified Rackett parameters for i

ρ_i = mass density of pure liquid i

$(MW)_i$ = component i, molecular weight.

For ethanol and water, the modified Rackett parameters given by Spencer and Danner are 0.2520 and 0.2380,

respectively.

c. Liquid Density Computer Implementation

In ETOH, the modified Rackett formula is used in determining liquid desities in subroutine TDEP(modeled after subroutine MVOL in the Prausnitz package). For a printout of the molar specific volumes MODE-24 should be set equal to 1 when the EtOH package is called.

d. Density Correlation--Critical Evaluation

Rackett correlation liquid density predictions are plotted along with measured densities for ethanol (4) and water (32) for temperatures up to near the fluid normal boiling points in Figure IIIA-4. The average errors for ethanol and water respectively are 0.0188 g/cm^3 and 0.0336 g/cm^3. For computation of the Poynting corrections to the vapor/liquid equilibrium equation, these accuracies are adequate. Further, the modified Rackett relations retain accuracy at elevated temperature (for up to $T/T_{ci} = 0.85$) and can be used in the design of supra-atmospheric pressure distillation systems.

For design at ordinary pressure, greater accuracy in the density specification may be necessary. For the temperature range of Figure IIIA-4, the simple numerical fits for ethanol (1) and water (33) may be used:

$$\rho_{ethanol} = 0.80632-0.00085365\ (T)-(10^{-8}(T)^2-2x10^{-9}(T^3) \quad (4-3)$$

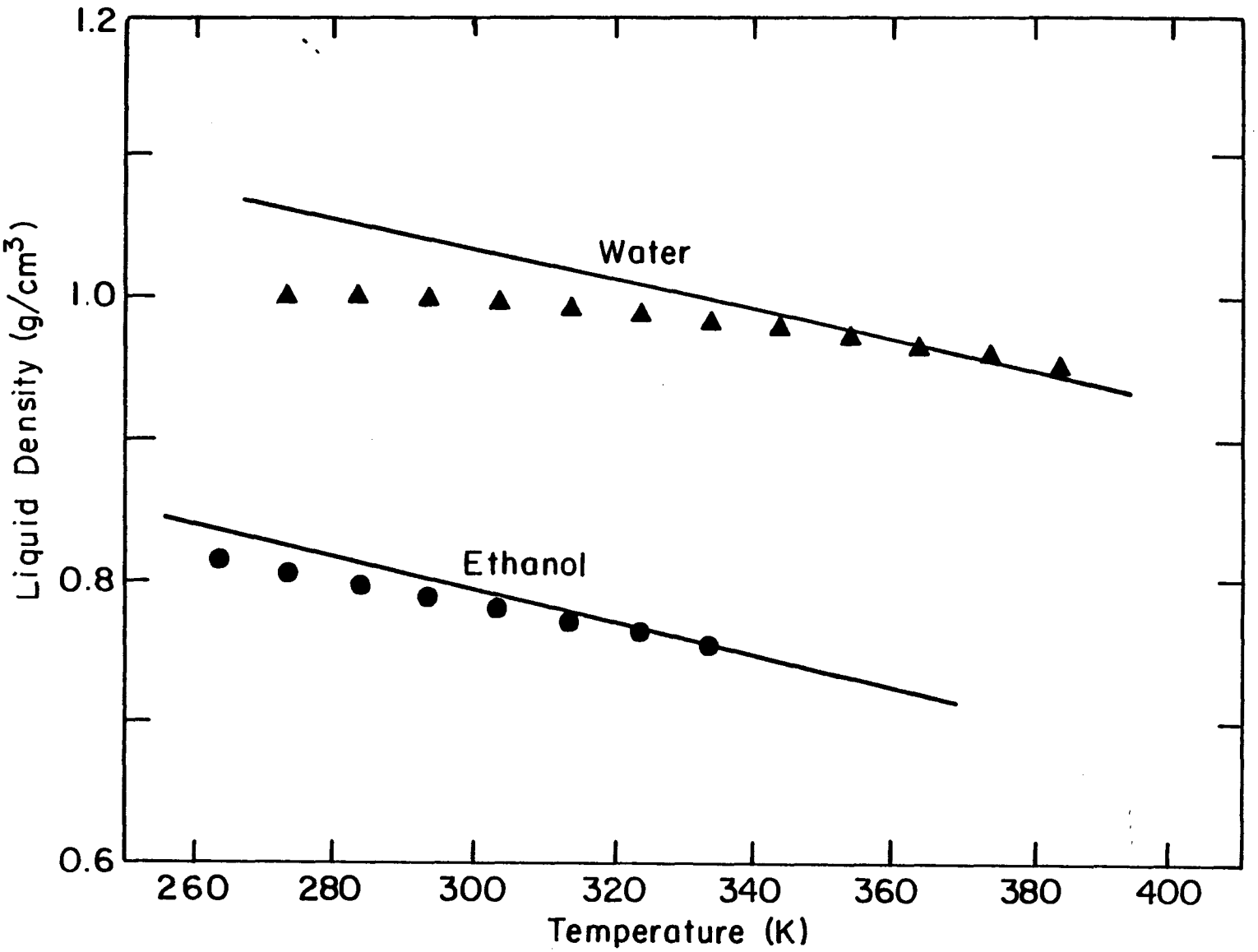

Figure IIIA-4. Measured liquid density versus temperature at ordinary pressure compared to calculated values from EQ. 4-3 and 4-4.

$$\rho_{water} = 1.0000326 + 2.3459\times10^{-5}(T) - 6.1070\times10^{-6}\times(T)^2 + 1.7334\times10^{-8}(T)^3 \quad (4\text{-}4)$$

$\rho \equiv gm/cm^3$ $\qquad$ $T \equiv {}^{o}C$

The ethanol density correlation reproduces the data with an average deviation of 0.00014. The maximum deviation for the water correlation is 0.00015.

5. Vapor Pressures and the Reference Fugacity

a. Vapor pressure correlations

Pure component vapor pressures are needed for design and also in establishing the liquid phase reference fugacities for vapor/liquid equilibrium determinations. The variation in pure component vapor pressure with temperature is given by the thermodynamically rigorous Clapeyron equation:

$$(d\ \ln P_{sat})/d(1/T) = \Delta H_{vap}/R(Z_{vap}-Z_{liq}) \quad (5\text{-}1)$$

where P_{sat} = pure component vapor pressure

T = temperature

R = ideal gas constant

ΔH_{vap} = heat of vaporization

Z = compressibility (PV/(RT))

Numerous vapor pressure correlations have been developed based on differing assumptions for the terms H_{vap} and $(Z_{vap}-Z_{liq})$ (not generally known appriori as functions of temperature (34-36). A detailed review is provided by Miller (37).

A particularly simple solution to the Clapeyron

equation (good over relatively small range of T) is the Antoine equation (38).

$$\ln P_{sat} = A - [B/(C+T)] \qquad (5\text{-}2)$$

Predictive methods have been devised for the Antoine constants (A,B,C), but these are best fit directly to experimental data (39).

b. Antoine correlation--critical evaluation

Antoine constants for ethanol and water at normal temperatures are given in Table IIIA-5. Figure IIIA-5 compares the correlation with the experimentally measured vapor pressure of Ambrose and Sprake (ethanol) (41) and the steam tables (water) (42). In both cases the fit is excellent and further refinements of the equations are not necessary. Antoine constants are also tabulated for most other typical solvents (5).

c. Zero Pressure Reference Fugacity Derivation

The general relation for vapor/liquid equilibrium may be expressed as:

$$Y_i \phi_i P^{total} = [X_i \gamma_i^{(T,P\ ref)}\ f_i^{0,liquid,\ P\ ref}] \exp[(P^{total}-P^{ref})V_i^{liq}/(RT)] \qquad (5\text{-}3)$$

where

$\gamma_i^{T,P\ ref}$ = liquid phase activity coefficient of component i at system temperature evaluated at reference pressure.

$f_i^{0,liq,\ P\ ref}$ = reference fugacity for component i in the

Table IIIA-5

Antoine Constants for Ethanol and Water (4, 5, 40)

Compound	Temp. Range	A	B.	C
Ethanol	0-100°C	18.91198	3803.99	231.48
Water	0-60°C	18,66855	4030.182	235.0
	60-150°C	18.34426	3841.20	228.0

For $\ln P_{sat} = A - \left(\frac{B}{C+T}\right)$

$P_{sat} \equiv$ mm Hg $T \equiv$ °C

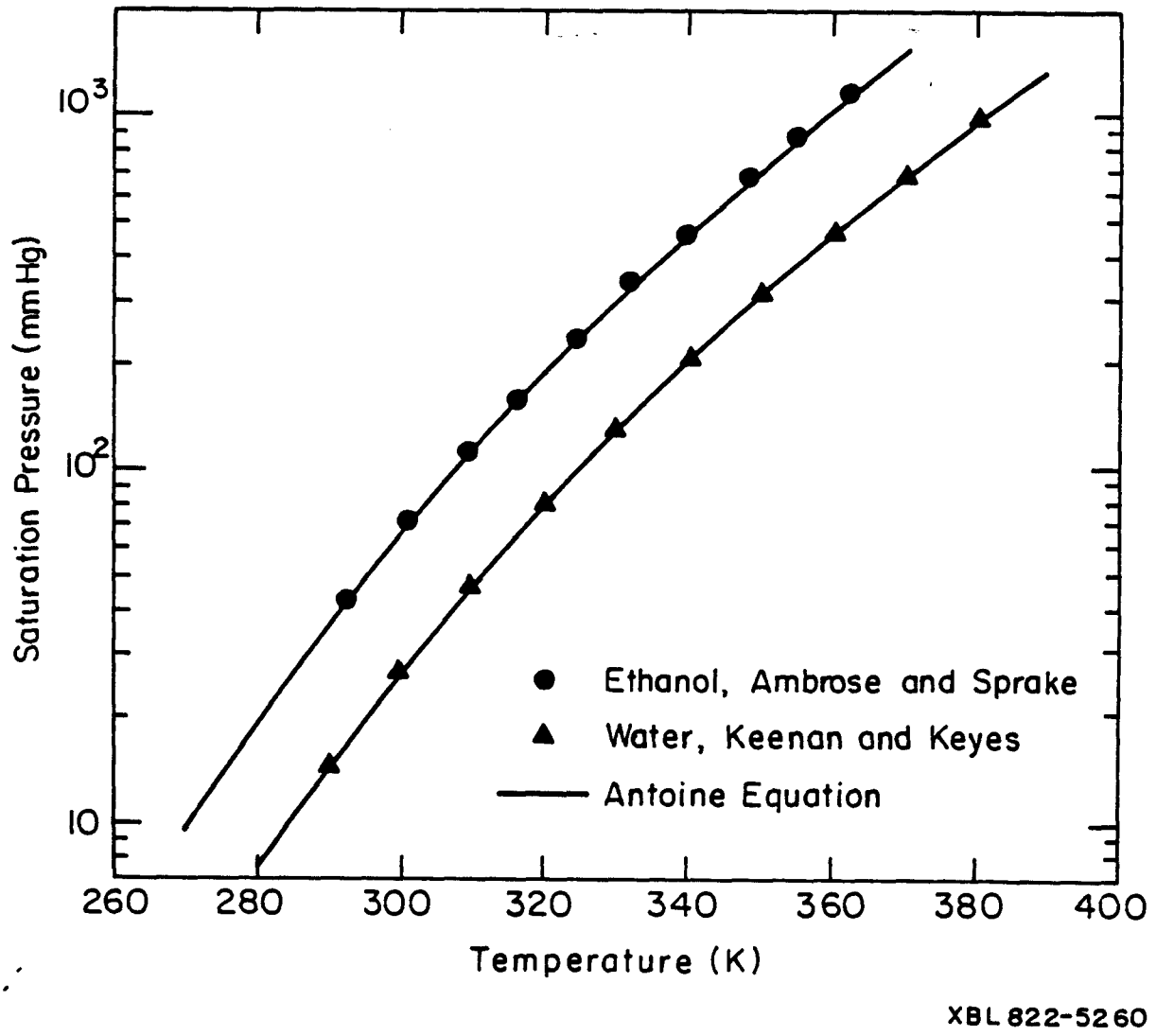

Figure IIIA-5. Measured values of saturation pressure of ethanol and water versus temperature compared to predicted curve by Antoine Equation.

liquid at the standard state conditions

(T, P^{ref}) of the activity coefficient.

A particularly convenient choice of reference pressure is $P^{ref} = 0$. This simplifies the Poynting correction term to

$$\text{Poynting correction} = \exp[(P^{total} V_i^{liq})/(RT)] \quad \text{(for P ref = 0)} \tag{5-4}$$

For this choice of reference pressure, it then follows (setting $X_i = Y_i = \gamma_i = 1$) that:

$$f_i^{0,liquid} = P^{sat} \phi_i^{sat} \exp[-(P_i^{sat} V_i^{liq}/(RT)] \tag{5-5}$$

where

$f_i^{0,liquid}$ = zero pressure reference fugacity for component i in the liquid

ϕ_i^{sat} = fugacity coefficient of component i, evaluated at system temperature and $P = P_i^{sat}$

d. Zero pressure reference fugacity correlation.

Having developed expressions for P_i^{sat}, ϕ_i^{sat} and V_i^{liquid} for ethanol and water, we can evaluate the zero pressure reference fugacity. For computational efficiency, Prausnitz has fit the reference fugacity directly to the form:

$$\ln f_i^{0,liq} = (C_{1,i}) + [(C_{2,i})/(T)] + [(C_{3,i})(T)] + [(C_{4,i})(\ln T)] + [C_{5,i})(T^2)] \tag{5-6}$$

In the normal temperature range this numerical fit is equivalent to evaluation of $f_i^{0,liq}$ according to equation 5-5. Further, at high pressures, the Lyckman correlation (43) was used to predict values of P_i^{sat} to insure reasonable values for $f_i^{0,liq}$ up to $T/(T_{ci}) = 1.8$. Extensive tables of constants for equation 5-6 have been compiled (6) and values for ethanol and water are presented in Table IIIA-6.

e. Reference fugacity-computer implementation

In ETOH, the reference fugacities are computed in subroutine TDEP(modeled after subroutine PURF in the Prausnitz package). Pure component vapor pressures can be generated using ETOH by calling BDPT with $X_1 = 1$ (ethanol) or $X_1 = 0$ (water).

f. Computer implementation--critical evaluation

Pure component vapor pressures generated by the EtOH package are presented in Table IIIA-7. The agreement with measured value (see Fig. IIIA-5)is excellent.

6. Future Accomplishments

Work has also been completed in evaluating and correlating:

1) ΔH_{mix} for ethanol and water
2) ΔH_{vap} for ethanol and water
3) C_p^{liq}, C_p^{vap} for ethanol and water
4) Solubility of CO_2, O_2, N_2
5) Heat of solution of CO_2, O_2, N_2
6) Activity coefficients for ethanol/water
7) Vapor/liquid equilibrium effects of

Table IIIA-6

Zero Pressure Reference Fugacity

Equation Constants

$$\ln f_i^{o,liquid} = C_{1,i} + \frac{C_{2,i}}{T} + C_{3,i}T + C_{4,i} \ln T + C_{5,i} T^2$$

	Ethanol	Water
C_i	-90.909919	57.041585
C_2	-3465.8735	-7004.8416
C_3	-0.062301392	0.003588444
C_4	20.486493	-6.66893878
C_5	2.0664221×10^{-5}	$-8.5054287 \times 10^{-7}$

Table IIIA-7

Computer Generated Pure Component Vapor Pressure

ETHANOL

Pressure (mm Hg)	Temperature (°K)	Pressure (mm Hg)	Temperature (°K)
19.0758	280.0000	7.4337	280.0000
26.4653	285.0000	10.4093	285.0000
36.2567	290.0000	14.3865	290.0000
49.0775	295.0000	19.6386	295.0000
65.6764	300.0000	26.4955	300.0000
86.9375	305.0000	35.3514	305.0000
113.8932	310.0000	46.6726	310.0000
147.7385	315.0000	61.0055	315.0000
189.8427	320.0000	78.9853	320.0000
241.7622	325.0000	101.3439	325.0000
305.2504	330.0000	128.9179	330.0000
382.2682	335.0000	162.6573	335.0000
474.9915	340.0000	203.6327	340.0000
585.8183	345.0000	253.0425	345.0000
717.3739	350.0000	312.2207	350.0000
872.5146	355.0000	382.6424	355.0000
1054.330	360.0000	465.9301	360.0000
1266.145	365.0000	563.8590	365.0000

fermentation by-product

8) Vapor/Liquid equilibrium effects of salts in fermenter beer

9) Vapor/Liquid equilibrium effects of yeast cells

10) Vapor/Liquid equilibrium correlations with various separating agents

This work will be summarized in a future report.

References

1. Prausnitz, J., T. Anderson, E. Grens, C. Eckert, R. Hsieh, J. O'Connell. Computer Calculations for Multicomponent Vapor-Liquid and Liquid-Liquid Equilibria. Prentice-Hall, Englewood Cliffs, N.J. (1980).

2. Weast, R.C., Handbook of Chemistry and Physics, 55th ed., CRC Press, Cleveland, Ohio (1974-1975).

3. Stecher, Paul G., The Merk Index, 8th ed., Merk Co., Rahway, N.J. (1968).

4. Pentz, C.A., "Ethanol," in Encyclopedia of Chem. Tech., 2nd ed., Kirk Othmer, Ed., McGraw-Hill, N.Y.

5. Reid, Robert, John M. Prausnitz, T.K. Sherwood, The Properties of Gases and Liquids, 3rd Ed., McGraw-Hill Co., N.Y. (1977).

6. Balzhiser, Richard E., M.R. Samuels, J.D. Eliassen, Chem. Eng. Thermodynamics, Prentice Hall, Englewood Cliffs, N.J. (1972).

7. Stogryn, D.E., J.O. Hirschfelder, J. Chem. Phys., 31 1531 (1959).

8. Singh, Y., S.K. Deb, A.K. Barna, J. Chem. Phys., 46, 4036 (1967).

9. Pitzer, K.S., J. Am. Chem. Soc., 79 2369 (1957).

10. Rigby, M., J. O'Connell, J.P. Prausnitz, Ind. Eng. Chem. Fund., 8, 460 (1969).

11. Hayden, J.G., J.P. O'Connell, "A Generalized Method for Predicting Second Virial Coefficients," Ind. Eng. Chem.

Proc. Des. Dev. Vol 14, No. 37 p. 209 (1975).

12. Hahn, R.L., L.I. Stiel, AIChE J., 17, 259 (1971).
13. Tee, L.S., S. Gatoh, W. Stewart, IEC Fund., 5(3), 356 (1966).
14. Johnson, J.R., P.T. Eubank, Ind. Eng. Chem. Fund. 12, 156 (1973).
15. O'Connell, J.P., J.M. Prausnitz, Ind. Eng. Chem. Proc. Des. Dev., 6, 245 (1967).
16. Nothnagel, K.H., D.S. Abrams, J.M. Prausnitz, Ind. Eng. Chem. Proc. Des. Dev. 12, 25 (1973).
17. Black, C., E.L. Perr, M.N. Papadopoulos, Ind. Eng. Chem., 55(9), 38 (1968).
18. Kreglewski, A., J. Phys. Chem., 73, 608 (1969).
19. Tsonopoulos, C., AIChE J., 20, 263 (1974).
20. Kretschmer, C.B., Wiebe, R., J. Am. Chem. Soc. 76 2579 (1954).
21. Lo, H.Y, L.I. Stiel, IEC Fund. 8, 713 (1969).
22. Knoebel, P.H., W.C. Edmister, J. Chem. Eng. Data 13, 312 (1968).
23. LeFevre, E.J., M.R. Nightingale, J.W. Rose, J. Mech. Eng. Sci., 17, 243 (1975).
24. Kell, G.S., G.E. McLaurin, E. Whalley, J. Chem. Phys., 48, 3805 (1968).
25. Keyes, F.G., L.B. Smith, H.T. Gerry, Proc. Am. Acad. Arts and Sci. 70, 319 (1936).
26. Tyn, M.T., W.F. Calus, Processing 21(4), 16 (1975).
27. Chueh, P.L., J.M. Prausnitz, AIChE J.13, 1099 (1967).

28. Gunn, R.D., T. Yamada, AIChE 17, 1341 (1971).

29. Yamada, T., R.D. Gunn, J. Chem. Eng. Data 18, 234 (1973).

30. Spencer, C.F., R.P. Danner, J. Chem. Eng. Data 17, 236 (1972).

31. Rackett, H.G., J. Chem. Eng. Data 15, 514 (1970).

32. Kell, G.S., J. Chem. Eng. Data 12, 67 (1967).

33. Maiorella, B.L., accepted for inclusion in Handbook of Chemistry, Lang, Editor, 13 ed., McGraw-Hill, N.Y.

34. Haggenmacher, J.E., J. Am. Chem. Soc. 68, 1633 (1946).

35. Frost, A.A., D.R. Kalwart, J. Chem. Phys.21, 264 (1953).

36. Thek, R.E., L.I. Stiel, AIChE J. 13, 626 (1967).

37. Miller, P.G., J. Phys. Chem. 68, 1399 (1964).

38. Antoine, C., C.R. 107, 681, 836 (1888).

39. Thompson, G.W., Techniques of Organic Chemistry, 3rd ed., Vol. 1, p.473, Interscience, N.Y. (1959).

40. Lange, N.A., Handbook of Chemistry, 10th ed., McGraw-Hill, N.Y. (1961).

41. Ambrose, D., C.S. Sprake, J. Chem. Thermo., 2, 631 (1970).

42. Keenan, J., F. Keyes, Thermodynamic Properties of Steam 1st ed., John Wiley and Sons, N.Y. (1936).

43. Lyckman, E.W, C.A. Eckert, J.M. Prausnitz, Chem. Eng. Sci. 20, 684 (1965).

B. Novel Ethanol-Water Separations

1. Introduction

As discussed in last year's report (5) on this subject, solvent extraction is being investigated as an alternative to distillation for ethanol recovery because there is a potential for significant energy savings. However, low distribution coefficients (the ratio of ethanol concentration in the solvent to that in the aqueous phase at equilibrium) or low separation factors (the ratio of ethanol distribution coefficient to water distribution coefficient) characterize most solvents that have been studied. Methods proposed to improve this situation include taking advantage of temperature effects in the ethanol-water solvent equilibria, the use of salts in the aqueous phase, and the use of complexing extractants and solvent mixtures.

2. Current Research

a) Temperature effects

As mentioned in last year's report (5), increasing extraction temperature increases the distribution coefficient of ethanol in the case of many solvents. This is reasonable since the activities of ethanol and water increase as their directional hydrogen bonds are weakened by random movement with the temperaure increase. Modelling of this behavior will be discussed in the Future Research section.

b) Salt effects in the aqueous phase

The salting out of solutes such as ethanol from aqueous solutions containing inorganic salts is well known. The

possibility of using this effect to enhance extraction recovery of ethanol was investigated. The effect is dependent on the specific salt used and on the concentration of the salt in the aqueous mixture. At the concentrations required for appreciable salting out, no salt could be used without recovery or recycle due to the cost of the salt itself. Direct recycle of the salt would be attractive if the fermentation could tolerate high salt concentrations. Experiments were performed using Saccharomyces cerevisae to test this idea.

Preliminary batch screening tests showed that the yeast could grow and ferment glucose in the presence of several salts at concentrations up to 1.0 molar. Of these, potassium chloride was selected for further study. The reason for choosing KCl was that the intracellular concentration of potassium ion is normally high (approximately 0.3 molar), and it was hoped that a high external concentration would have less effect on cell metabolism than other salts. The salting out of ethanol from fermentation broth by KCl was confirmed in batch equilibrium tests with selected solvents. In 1.0 molar KCl, the distribution coefficient of ethanol of approximately 5 wt% was increased by a factor of 1.5. The salting coefficient, k_s, as defined by Johnson and Furter (1) is 8.2 for this case, higher than the value of 4.2 reported by them for KCl at higher ethanol concentrations.

The results of continuous fermentation studies with 1.0 molar KCl in the feed, however, were not encouraging for this system. With a low feed concentration (20 g/L glucose) and low

dilution rate (0.06 hr^{-1}), the salt-containing fermentation showed a slightly lower ethanol yield than a control fermentation, 0.38 g. EtOH/g.glucose versus 0.42 g.EtOH/g.glucose. However, when ethanol was added to the feed so that the fermentor alcohol concentration was 30 g/L, the ethanol yield of the salt-containing fermentation dropped to 0.18 g.EtOH/g.glucose consumed. The control fermentation with 30 g/L of ethanol in the fermentor showed less of a yield decrease, to 0.34 g EtOH/g.glucose consumed. Apparently, as the salt increases the activity of the ethanol, the combination of salt and ethanol in the mixture has more profound metabolic effects than either alone. If confirmed by future work, these results clearly show that a potassium chloride-containing fermentation for ethanol production will not work well for this organism.

c) Complexing extractive agents

Experiments were done to test the hypothesis discussed in last year's report that electrophilic, Lewis acid, or H-donor compounds should show good ethanol-selective extractant properties. In one experiment, three compounds representing three types of extractive agents were tested under similar conditions. The compounds were trioctylphosphine oxide (TOPO), which is capable of forming hydrogen bonds only with hydrogen atoms of the -OH groups of ethanol or water, pentachloroethane which can form hydrogen bonds only with the oxygen atom of the -OH groups of ethanol or water and 1-dodecanol which can form either kind of hydrogen bonds. All three were dissolved in tetradecane to a concentration of 0.22 M. This was

necessary for TOPO, which is a solid at ambient temperature, and was done for the others to afford direct comparison. Each solution was equilibrated with dilute aqueous ethanol (approximately 5 wt%), and distribution coefficients were measured. The results are given below:

EXTRACTANT	$K = \frac{\text{wt\% EtOH Organic}}{\text{wt\% EtOH Aqueous}}$
TOPO in tetradecane	0.13
1-dodecanol in tetradecane	0.02
pentachloraethane in tetradecane	0.008
pure tetradecane	0.005

Evidently, the type of hydrogen bond formed is not as important for ethanol extraction as the strength of the bond. The latter is presumably determined by the dipole moment of the extractive agent in this case. A possible complication exists in that the extractive agents are of different sizes, with different moments of inertia. Because of this, they may be rotating in solution at different rates which affect their ability to hydrogen bond with ethanol or water. Further work in this area will involve using a greater size range of compounds and determining separation factors as well as distribution coefficients.

d) Solvent mixtures

There are a number of solvent mixtures which are of interest as extractive agents because varying the proportions of their components controls distribution and selectivity for ethanol. An example, which has been investigated experimentally, is the 1-dodecanol-tetradecane system. In this system, at 25°C, the ethanol distribution coefficient varies nearly linearly with

weight fraction of dodecanol, from 0.005 for pure tetradecane to 0.30 for pure dodecanol. The separation factor varies such that the weight fraction of ethanol on a solvent free basis in the organic phase [EtOH org./(EtOH + H_2O) org.] in equilibrium with approximately 6 wt% aqueous ethanol also varies linearly. It drops from 0.87 for pure tetradecane to 0.45 for pure dodecanol. An optimal extraction solvent for this system could be obtained by using these data in appropriate process models with economic anaysis.

3. Future Work

It would be of considerable practical advantage to be able to model the phase equilibrium behavior of ethanol-water-extractants and to predict the behavior for untested extractants. This is the goal of the next phase of this work. To begin, the UNIQUAC equaton will be used because it has proven quite successful in the prediction of many liquid-liquid equilibria. The procedure used is that given by Prausnitz, et al. (2), and the computer programs used are essentially the same as those published in that work.

The details of the UNIQUAC equation were given in last year's report (5) as it is being used by Maiorella to model the vapor-liquid equilibria of ethanol-water. The key parameters in the model are binary interaction parameters A_{ij} and A_{ji} which must be known for every pair of components in the system. As a result of Maiorella's work, the binary interaction parameters for ethanol-water are known as a function of temperature. This gives

the potential for more accurate prediction of liquid-liquid equilibria as a function of temperature. The binary interaction parameters for water-extraction solvent pairs have been fitted (for many pairs of interest) by Sorensen and Arlt (3) from mutual solubility data. This leaves the binary interaction parameters of the ethanol-solvent pairs to be determined. It is these parameters which will be fit using the equilibrium data obtained from experiments. The fitted parameters will be compared with the predictions of UNIFAC, a group contribution method, which has recently been updated for liquid-liquid equilibria by Magnussen, et al. (4). An interesting aspect of this work will be the use of parameters for ethanol-water-pure solvent systems to predict the equilibrium behavior in ethanol-water-mixed solvent systems such as the dodecanol-tetradecane extractant system, which was discussed previously.

References

1. Johnson, A and W. Furter, Can. J. Chem. Eng. 38, 78 (1960).

2. Prausnitz, J., T. Anderson, E. Grens, C. Eckert, R. Hsieh, and J. O'Connell, Computer Calculations for Multicomponent Vapor-Liquid and Liquid-Liquid Equilbria (1980). Prentice-Hall.

3. Sorensen, J. and W. Arlt, Liquid-Liquid Equilibrium Data Collection (1979). DECHEMA.

4. Magnussen, T., P. Rasmussen, and A. Fredenslund, "UNIFAC Parameter table for Prediction of Liquid-Liquid Equilibria," Ind. Eng. Chem. Process. Des. Dev. 20, 331 (1981).

5. Wilke, C.R., H.W. Blanch, "Bioconversion of Cellulose,"

Univ. of California, Berkeley, LBL-12602 (March 1981), 1980 Progress report to D.O.E., Division of Basic Energy Sciences.

This work was supported by the Director, Office of Energy Research, Office of Basic Energy Sciences, Division of Chemical Science Processes and Techniques Branch of the U.S. Department of Energy under Contract Number DE-AC03-76SF00098.

APPENDIX

BIOCONVERSION OF CELLULOSE AND PRODUCTION OF ALCOHOL

Project Staff

Faculty Investigators

Charles R. Wilke, Professor of Chemical Engineering
Harvey W. Blanch, Associate Professor of Chemical Engineering

Post-Doctoral Investigators

Neil Hendy

Graduate Students

1. Ph.D. Candidates

Brian Maiorella
Kevin Murphy
Bruce Vick Roy
Dale Wiley
Harry Wong

2. MS Candidates

Betsy Elzufon
Tony Mancusco
Steven Orichowsky

3. Support Staff

Aldo F. Sciamanna, Senior Chemist

RESEARCH PROGRAM AND PERSONNEL

February 1982

Fundamental and Process Development Studies on the Bioconversion of Cellulose and Production of Ethanol

Faculty Investigators

Charles R. Wilke, Professor of Chemical Engineering
Harvey W. Blanch, Assosicate Professor of Chemical Engineering

Department of Energy--Basic Energy Sciences Division

(FY82 Funding, $107,000)

I. Studies on the Mechanism and Kinetics of Cellulose Hydrolysis

A. Kinetic and Mechanistic Studies on Cellulase Enzymes (Dale Wiley)

B. International Cooperative Measurement of Cellulase Enzyme Activity (Aldo F. Sciamanna)

II. Fundamental Studies of High Productivity Fermentations

A. Basic Studies on Yeast Nutrition (Harry Wong)

B. Models of Yeast Growth and Ethanol Inhibition (Harry Wong)

C. By-Product Inhibition in Cell Recycle and Vacuum Fermentation (Brian Maiorella)

D. Hollow Fiber Reactor (Bruce Vick Roy)

III. Fundamental Studies on Product Recovery

A. Ethanol Water Physical Chemical Properties (Brian Maiorella)

B. Novel Ethanol-Water Separations (Kevin Murphy)

Research Program and Personnel continued

Department of Energy-Solar Energy Research Institute, Golden, Colorado (FY82 $200,000)

I. Process Development Studies

A. Economic Evaluation of Flash-Fermentation and Distillation (Brian Maiorella)

B. Raw Materials Evaluation (Aldo Sciamanna)

C. Evaluation of Pretreatment Processes (Aldo Sciamanna)

II. Microbiological and Enzymatic Studies

A. Production of Cellulase Enzyme from High Yielding Mutants (Neil Hendy)

B. Hydrolysis Reactor Development

1. Countercurrent Hydrolysis Reactor Development (Steven Orichowsky)

C. Fermentation of Xylose (Tony Mancusco)

III. Fermentation and Separation Processes

A. Process Development Studies on Vacuum Fermentation and Distillation (Brian Maiorella)

B. Evaluation of Low Energy Separation Processes (Kevin Murphy)

C. Large Scale Hollow Fiber Reactor Development (Bruce Vick Roy)

Research Program and Personnel Continued

Center for Biotechnology

Funding for 4 years, $789,000

6 graduate students

National Science Foundation, Engineering Division

"Mass Transfer and Thermodynamics FY 1982 $43,505

3 graduate students

BES Review 1982
Publications

1. Castanon, Marisi and Charles R. Wilke, "Effects of the Surfactant Tween 80 on Enzymatic Hydrolysis of Newsprint," Biotechnol. Bioeng. 23, 1365 (1981).

2. Wilke, C.R. and B. Maiorella, "High Productivity Anaerobic Fermentation with Dense Cell Culture," Proceedings of VIth Intern'l Symposium and Vth Intern'l Symposium on Yeasts, July 20-25, 1980, London, Ontario, Canada (1981).

3. Maiorella, B., C.R. Wilke and H.W. Blanch, "Alcohol Production and Recovery," Advances in Biochemical Engineering 20, Bioenergy, 43, Springer-Verlag, Berlin, Heidelberg, New York (1981).

Pending Publications

Blanch, H.W. and C.R. Wilke, "Sugars and Chemicals from Cellulose," Reviews in Chemical Engineering, Amndsen, N.E., and Luss, D., Editors.

Maiorella, B., H.W. Blanch and C.R. Wilke, "By-Product Inhibition on Ethanolic Fermentation by Saccharomyces cerevisiae," Biotech. Bioeng, Symp. Series (1982).

Hendy, N., C.R. Wilke and H.W. Blanch, "Enzymatic Hydrolysis" Chapter in Biomass Conversion Handbook. John Wiley & Sons, New York (1982).

Wiley, D., C.R. Wilke and H.W. Blanch, "Enzymatic Hydorlysis" Chapter in Biomass Conversion Handbook. John Wiley & Sons, New York (1982).

Papers Presented at Meetings

By-Product Inhibition Effects on Ethanolic Fermentation by Saccharomyces cerevisiae, American Chemical Society, New York, August 1981. (presented by Brian Maiorella) Received Peterson Award.

Bioconversion of Cellulose and Production of Ethanol, Solar Energy Research Inst. Washington, D.C., November 1981. (presented by H.W. Blanch)

Papers Presented at International Meetings

Water Recycle in Extractive Fermentation, First Engineering Foundation Conf., Advances in Fermentation Recovery Process Technology," Banff, June 1981. (presented by Kevin Murphy)

Enzymatic Conversion of Cellulosic Materials for Fuels and Chemical Production, Enzyme Engineering Conf. VI, Kashikojima, Japan, September 20-25, 1981.

Applied Biotechnology, Lecture Series. Presented at Institute Polytecnico, Nacional Escuela Nacional de Ciencias Biologicas, Mexico, February 1982.

Lectures

"Bioconversion of Cellulose," Dept. of Chem. Engineering, Univ. of California, San Diego, November 1980.

Bioconersion of Cellulosic Materials to Ethanol, Dept. of Chemical Engineering, University of California, Davis. February 1981.

Lawrence Berkeley Laboratory Reports

1. Wilke, C.R., H.W. Blanch, K. Tangnu, D. Wiley, B. Long, S. Rosenberg, J.-P Riba, and L. Sindalar, "Enzymatic Conversion of Wood and Agricultural Residues to Sugars, Lawrence Berkeley Laboratory Report, Chemical Process Research and Development Program, Chapter from the Energy and Environmental Development Division Annual Rept. 1980, LBL-11983, March 1981.

2. Wilke, C.R., H.W. Blanch, B. Maiorella, K. Murphy, B. Vickroy and H. Wong, "Ethanol Production and Recovery from Biomass Sugars, Chemical Process Research and Development Program, Chapter from the Energy and Environment Division Annal Report 1980, LBL-11983, March 1981.

3. Wilke, Charles R. and Harvey W. Blanch, "Process Development Studies on the Bioconversion of Cellulose and PRODUCTION OF Ethanol, LBL-12603.

4. Maiorella, Brian, Harvey W. Blanch and Charles R. Wilke, "Bi-Product Inhibition of Ethanolic Fermentation by Saccharomyces cerevisiae," LBL-12603

5. Wilke, Charles R., Brian Maiorella, Aldo F. Sciamanna, Kishen Tangnu, Dale Wiley, and Harry Wong, "Enzymatic Hydrolysis of Cellulose Theory and Applications, Workship on the cooperative Research Project of Food Production, Preservation and Conversion of Lignocellulosic Waste Products. Sponsored by the Organization for Economic cooperation and Development, Paris, France, June 1980, LBL-13669, June 1980.

Thesis Completed (Pending LBL Reports)

George Brown Dove, III, MS Degree, "Process Development Studies for the Enhanced Recovery of Cellulase in Cellulose Hydrolysis, 1981.

Robert Alexander Antonoplis, MS Degree, High Pressure Conversion of Cellulose to Glucose," 1981.

Stephen Alan Wald, "Enzymatic Hydrolysis of Rice Straw for Ethanol Production, MS Degree, 1981.

Thomas A. Delfino, "Conversion of Xylose to Ethanol by Bacillus macerans," MS 1981.

Javier Perez, "Enzymatic Hydrolysis of Corn Stover: Process Development and Evaluation, MS 1981.